Geological Society of America Bulletin

The Paleocene–Eocene thermal maximum (PETM) in shallow-marine successions of the Adriatic carbonate platform (SW Slovenia)

Jessica Zamagni, Maria Mutti, Paolo Ballato and Adrijan Kosir

Geological Society of America Bulletin 2012;124, no. 7-8;1071-1086
doi: 10.1130/B30553.1

Notes

The Paleocene–Eocene thermal maximum (PETM) in shallow-marine successions of the Adriatic carbonate platform (SW Slovenia)

Jessica Zamagni[1,†], Maria Mutti[1,†], Paolo Ballato[1,†], and Adrijan Košir[2,†]
[1]*Institut für Erd- und Umweltwissenschaften, Universität Potsdam, Karl Liebknecht Strasse 24, D-14476 Golm, Potsdam, Germany*
[2]*Ivan Rakovec Institute of Palaeontology, Research Centre of the Slovenian Academy of Science & Arts (ZRC SAZU), Novi trg 2, SI-1000 Ljubljana, Slovenia*

ABSTRACT

The Paleocene-Eocene thermal maximum represents one of the most rapid and extreme warming events in the Cenozoic. Shallow-water stratigraphic sections from the Adriatic carbonate platform offer a rare opportunity to learn about the nature of Paleocene-Eocene thermal maximum and the effects on shallow-water ecosystems. We use carbon and oxygen isotope stratigraphy, in conjunction with detailed larger benthic foraminiferal biostratigraphy, to establish a high-resolution paleoclimatic record for the Paleocene-Eocene thermal maximum. A prominent negative excursion in $\delta^{13}C$ curves of bulk-rock (~1‰–3‰), matrix (~4‰), and foraminifera (~6‰) is interpreted as the carbon isotope excursion during the Paleocene-Eocene thermal maximum. The strongly ^{13}C-depleted $\delta^{13}C$ record of our shallow-marine carbonates compared to open-marine records could result from organic matter oxidation, suggesting intensified weathering, runoff, and organic matter flux.

The Ilerdian larger benthic foraminiferal turnover is documented in detail based on high-resolution correlation with the carbon isotopic excursion. The turnover is described as a two-step process, with the first step (early Ilerdian) marked by a rapid diversification of small alveolinids and nummulitids with weak adult dimorphism, possibly as adaptations to fluctuating Paleocene-Eocene thermal maximum nutrient levels, and a second step (middle Ilerdian) characterized by a further specific diversification, increase of shell size, and well-developed adult dimorphism. Within an evolutionary scheme controlled by long-term biological processes, we argue that high seawater temperatures could have stimulated the early Ilerdian rapid specific diversification. Together, these data help elucidate the effects of global warming and associated feedbacks in shallow-water ecosystems, and by inference, could serve as an assessment analog for future changes.

INTRODUCTION

The Paleocene-Eocene transition is marked by global warming corresponding to one of the warmest periods of the Cenozoic, culminating with the early Eocene climatic optimum (Zachos et al., 2001). The maximum warming episode of this period is known as the Paleocene-Eocene thermal maximum, an abrupt and short-lived spike in global temperatures. During the Paleocene-Eocene thermal maximum, sea temperatures increased by 4–8 °C. The Paleocene-Eocene thermal maximum was associated with a negative carbon isotope excursion, expressed in marine carbonates by a >2.5‰ excursion (e.g., Kennett and Stott, 1991; Bains et al., 1999; Thomas et al., 2002; Zachos et al., 2003; Tripati and Elderfield, 2005). The duration of the main body of this excursion has been estimated to be ~100 k.y. (e.g., Röhl et al., 2000, 2007; Giusberti et al., 2007). The carbon isotope excursion has been related to a geologically instantaneous (<10 k.y.) injection of ^{13}C-depleted carbon in the form of CO_2 and/or CH_4 into the global exogenic carbon pool (Dickens et al., 1995, 1997). The mechanism that triggered this release, however, remains controversial (Zachos et al., 2008).

The Paleocene-Eocene thermal maximum is widely known from pelagic, hemipelagic, and continental records. Studies on the effects of the Paleocene-Eocene thermal maximum in open-marine ecosystems document heterogeneous responses ranging from dramatic extinction (deep-sea benthic foraminifera extinction; e.g., Thomas, 2007) to rapid spreading (global acme of the heterotrophic dinocyst *Apectodinium*; e.g., Bujak and Brinkhuis, 1998; Crouch et al., 2001; Egger et al., 2003). Investigations of marine sequences from continental outer shelves have found evidence for increased seawater temperature, runoff, and productivity in coastal oceans during the Paleocene-Eocene thermal maximum (e.g., Gibson et al., 1993; Bujak and Brinkhuis, 1998; Egger et al., 2003; Gibbs et al., 2006; Sluijs and Brinkhuis, 2009), pointing to an important perturbation of the nutrient cycle. This eutrophication, however, has not been globally documented in open-ocean settings (e.g., Gibbs et al., 2006, and references therein).

Shallow coastal waters are key locations to link continental and open-marine settings in order to better understand the nature and intensity of the environmental changes and biological responses associated with the Paleocene-Eocene thermal maximum. However, studies on such environments have been limited due to the lack of adequate sections covering this time interval. Previous studies on the Paleocene-Eocene thermal maximum in shallow-water successions from the Pyrenean basin (Spain) (Orue-Etxebarria el al., 2001; Pujalte et al., 2003a, 2009) and the Galala Mountains (Egypt) (Scheibner et al., 2005; Scheibner and Speijer, 2009) attempted to establish a temporal correlation between the evolution of larger benthic foraminifera and the Paleocene-Eocene thermal maximum. Because larger benthic foraminifera are very sensitive to seawater physical-chemical composition (e.g., nutrient/sediment load and seawater pH; e.g., Hallock et al., 2003), changes observed among these organisms can be used to reconstruct past paleoenvironmental conditions. This group of biocalcifiers showed a diversification around the Paleocene-Eocene transition associated with the development of adult dimorphism and large shell size, which occurred at the base of the Ilerdian stage (Hottinger and Schaub, 1960; Hottinger, 1998). Studies conducted in the Pyrenees and Egypt concluded that this evolutionary change, defined as the

[†]E-mails: zamagni@geo.uni-potsdam.de; mmutti@geo.uni-potsdam.de; ballato@geo.uni-potsdam.de; adrijan@zrc-sazu.si

GSA Bulletin; July/August 2012; v. 124; no. 7/8; p. 1071–1086; doi: 10.1130/B30553.1; 8 figures; Data Repository item 2012212.

larger foraminifera turnover (Orue-Etxebarria el al., 2001), correlates with and was causally linked to the Paleocene-Eocene thermal maximum (Orue-Etxebarria et al., 2001; Pujalte et al., 2003a; Scheibner et al., 2005). Uncertainties in the correlation persist, however, because the record of larger foraminifera is not continuous across the Paleocene-Eocene thermal maximum event in these regions, due to the presence of important facies changes. More recent data from Ocean Drilling Program (ODP) Site 871 in Pacific Ocean guyot (Robinson, 2011) show no evidence of a biocalcification crisis associated with the Paleocene-Eocene thermal maximum. At that site, however, the Paleocene-Eocene thermal maximum is not fully recorded due to core recovery gaps and low biostratigraphic resolution. An accurate correlation between the carbon isotopic excursion associated with the Paleocene-Eocene thermal maximum and the evolution of the larger benthic foraminifera therefore remains elusive. The fundamental prerequisite to tackle the issue about the nature of Paleocene-Eocene thermal maximum and the effects on shallow-water ecosystems is the identification of fully marine carbonate sections deposited in shallow-water settings with a well-defined record of the Paleocene-Eocene thermal maximum and in situ larger benthic foraminifera in sufficient abundance to perform high-resolution biostratigraphy.

In this study, we present new carbon and oxygen isotopic data from the Adriatic carbonate platform, SW Slovenia. Here, the combination of continuous sedimentation of thick, shallow-water marine carbonate deposits spanning the critical interval of the late Paleocene–early Eocene and the high abundance of index fossils (Drobne, 1977; Zamagni et al., 2008) offers the rare opportunity to perform a high-resolution study documenting (1) the isotopic expression of the Paleocene-Eocene thermal maximum for in situ shallow-water marine carbonates; and (2) the effects of the Paleocene-Eocene thermal maximum on shallow-water systems, particularly the responses of larger benthic foraminifera. Our results highlight the potential of the successions from the Adriatic carbonate platform to serve as a paleoclimatic archive, representing one of the most complete shallow-water marine successions across the Paleocene-Eocene boundary with a detailed record of the event.

GEOLOGICAL AND STRATIGRAPHICAL SETTING

The studied carbonate platform successions are exposed in the southern part of the Kras (Karst) Plateau in SW Slovenia (Fig. 1A) within the NW External Dinaric fold-and-thrust belt. The Kras area corresponds to the northwestern part of the Adriatic carbonate platform, an isolated platform located along the northern margin of the Tethys (Fig. 2). During the latest Cretaceous–early Paleogene, the area was characterized by a relatively narrow belt of carbonate platform depositional systems on the southwestern margin of a NW-SE–trending foreland basin (Košir, 1997; Zamagni et al., 2008). The uppermost Cretaceous to Eocene carbonate succession was deposited during major tectonic events when a large part of the platform was subaerially exposed, re-established, drowned, and finally buried by prograding deep-water clastics (flysch).

The upper part of the carbonate sequence in the Kras region corresponds to the Kras Group (Košir, 2003; Fig. 1B), which overlies the forebulge unconformity and consists of three formations: (1) the Liburnian Formation (Upper Maastrichtian to Lower Paleocene), characterized by restricted, marginal marine and paralic carbonates; (2) the Trstelj Formation (Upper Paleocene), composed of a lower member dominated by foraminiferal limestones, and an upper member including foralgal/coralgal limestones and microbialite-coral mounds; and (3) the Alveolina-Nummulites Limestone (Lower Eocene), dominated by accumulations of larger benthic foraminifera (Zamagni et al., 2008, 2009) (Fig. 1B). The total thickness of the Kras Group ranges from several tens of meters to more than 450 m (Jurkovšek et al., 1996; Jurkovšek, 2010), and it is overlain by Transitional Beds (Lower Eocene) consisting of up to 50 m of pelagic and hemipelagic limestones and marls. The uppermost unit (flysch; Lower Eocene) is composed of a thick succession of sandstone-dominated turbidites, marls, mudstones, and resedimented carbonates. Regional facies relationships and facies successions (Zamagni et al., 2008, and references therein) point to carbonate ramp depositional systems characterized by roughly parallel NW-SE–trending facies belts. The studied area constitutes the thickest and the most complete record of the early Paleogene on the Adriatic carbonate platform.

METHODOLOGY

Sections and Biostratigraphy

The studied successions are exposed along the motorway between Postojna and Koper (Fig. 1). Two main sections, Čebulovica and Kozina, were sampled in detail for biostratigraphic and chemostratigraphic studies (Figs. 1C–1D). Several shorter sections (Divača, Divača-Kozina East, and Divača-Kozina West; Fig. 1A) were logged to refine the facies and biostratigraphic data set. All the sections show moderate tectonic deformation and almost continuous exposure. The Čebulovica section is 200 m thick and is composed of 155 m of poorly bedded to massive limestones of the Trstelj Formation, overlain by 45 m of thick, wavy-bedded Alveolina-Nummulite Limestones. The Kozina section is 100 m thick and consists of 50 m of thick-bedded to massive limestones of the Trstelj Formation, overlain by 50-m-thick Alveolina-Nummulite Limestones. We logged, sampled, and described the sections with respect to the sedimentary structures and components. Samples were collected at an average interval of 20 cm for both the Čebulovica and Kozina sections. We analyzed 350 thin sections for microfacies and microfossil content, with special emphasis on larger benthic foraminifera. We estimated components semiquantitatively and summarized them in Table DR1,[1] together with the main sedimentary/diagenetic features, foraminiferal assemblages, and interpretation of the depositional settings. Textural and compositional characteristics of the investigated lithologies were based on transmitted-light microscopy.

The biostratigraphic correlation of the studied sections is based on the distribution and biozonations of larger benthic foraminifera (Fig. 3). Taxonomic identification of foraminifera is based on Drobne (1977), Hottinger (1960), Schaub (1981), and Hottinger and Drobne (1980). All the species used in this work represent index fossils of the Tethyan Shallow Benthic Zonation established by Hottinger (1960) and revised by Serra-Kiel at al. (1998).

Carbon and Oxygen Isotope Analysis

The application of chemostratigraphy to rocks from shallow-water settings requires some considerations. Particularly, the degree of stratigraphic resolution attained is related to (1) the quality of the data set (bulk-rock vs. single-component analysis), (2) the preservation of original marine signatures and, therefore, the extent and nature of diagenetic processes, and (3) "vital effects" of organisms that may fractionate isotopes during biocalcification (especially carbon isotopes; see Langer, 1995, and references therein).

With the aim of obtaining the highest-resolution chemostratigraphic record in the studied

[1]GSA Data Repository item 2012212, Figure DR1 and Tables DR1–DR4, is available at http://www.geosociety.org/pubs/ft2012.htm or by request to editing@geosociety.org.

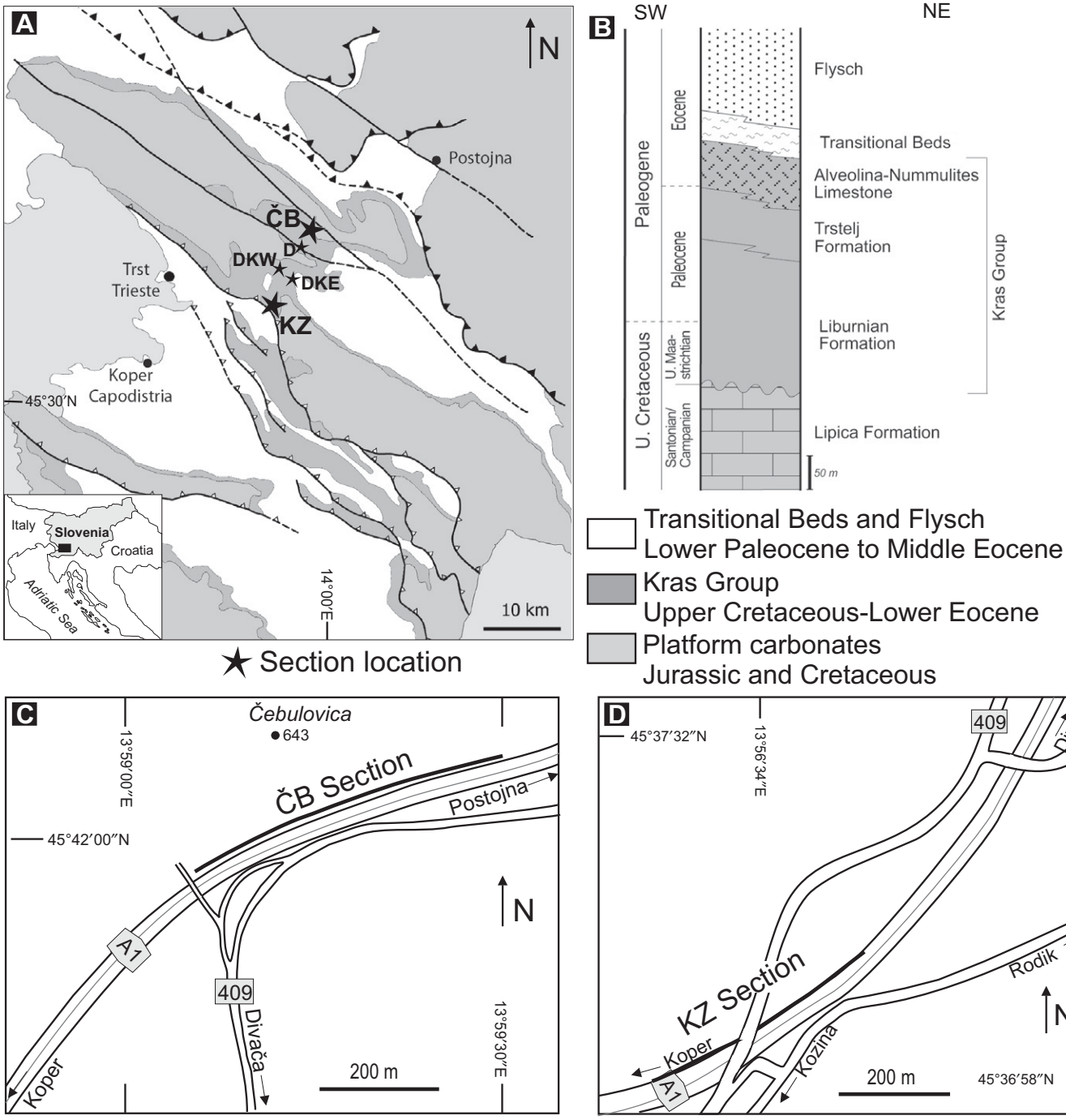

Figure 1. Geographic and geological context of the study area. (A) Simplified geological map of SW Slovenia and NW Croatia modified from Košir (2003). (B) Stratigraphic column of the uppermost Cretaceous–Eocene succession in the Kras region (Košir, 2003). (C) Location of the Čebulovica section. (D) Location of the Kozina section. Section labels: KZ—Kozina; ČB—Čebulovica; D—Divača; DKE—Divača-Kozina East; DKW—Divača-Kozina West.

material, we first analyzed the bulk-rock values across the entire succession. These measurements provided a first-order framework of the variability of the data sets, which allowed us to evaluate diagenetic effects and possible facies dependency. In total, 357 samples were processed. Samples for isotope stratigraphy were taken at an average spacing of ~1 m, except for the Paleocene-Eocene boundary, where the sample spacing was ~30 cm in the Čebulovica section, and ~50 cm in the Kozina section. Following this first step, in an attempt to produce reliable high-resolution $\delta^{13}C$ curves, we sampled the stratigraphically critical intervals for single-component isotopic analysis. In the Čebulovica section, fine-grained and texturally uniform matrix, large miliolids/alveolinids, and nummulitids were sampled for stable

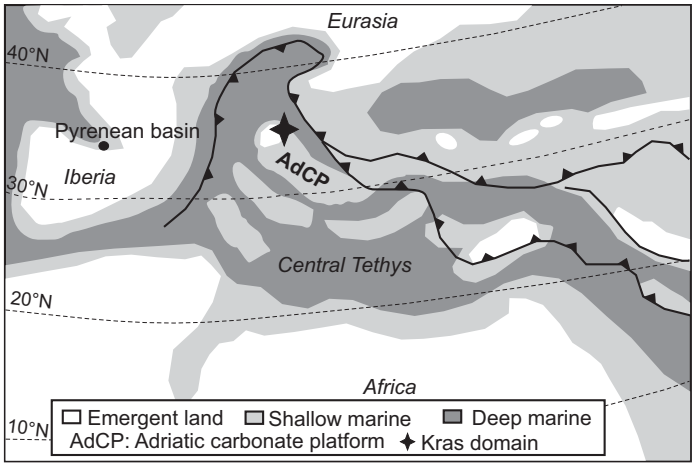

Figure 2. Early Paleogene paleogeographic reconstruction based on Ziegler (1990) with the approximated location of the Kras domain (black star) and the Pyrenean basin (black point).

isotope analysis close to the Paleocene-Eocene boundary. Powder samples were obtained by microdrilling polished slabs under a binocular microscope, taking care to avoid cement-filled veins and pores, larger bioclasts, and cement within the foraminiferal chambers. The bulk samples were analyzed by a ThermoFisher DELTA plus XL GasBench II mass spectrometer at the GeoForschungsZentrum (GFZ) in Potsdam. The matrix and foraminiferal samples were analyzed by a ThermoFischer MAT 253 GasBench II at the ETH in Zurich. Stable isotope values were calculated with respect to the Vienna Peedee belemnite (VPDB) scale. Replicate analysis of standards (NBS19, CO1, CO8) indicated a precision of ±0.1‰.

RESULTS

Facies and Depositional Model

Based on field data and thin-section analysis, we defined 18 lithofacies organized into three facies associations (Zamagni et al., 2008). The main compositional and textural features of each facies are summarized in Table DR1 (see footnote 1). The evolution of the depositional system and the facies models are presented in Figure DR1 (see footnote 1). The Upper Paleocene deposits (Trstelj Formation) comprise facies association A, which consists of the foraminiferal limestones (SBZ3, early Thanetian), and facies association B, which consists of the foralgal limestones (SBZ4, late Thanetian). Facies association A is composed of a suite of facies deposited in innermost ramp environments, including restricted lagoonal and paralic carbonates. Locally, levels with in situ and reworked *Microcodium* and typical calcrete microfeatures (alveolar septal structure, micrite coatings and cements, circumgranular crackings and peloids, microbrecciation, rhizoliths) indicate short episodes of subaerial exposure and early stages of soil formation (Košir, 2004). The transition to facies association B is marked by a shift to lime matrix-dominated lithologies deposited in inner to midramp settings. Lower Eocene limestones (Alveolina-Nummulites Limestone), comprising facies association C (biopeloidal limestones, SBZ5–SBZ8, early–middle Ilerdian), were mostly deposited in inner to midramp settings dominated by larger benthic foraminifera. In all studied sections, facies association C is characterized by a wavy, pseudonodular bedding pattern. Well-cemented parts, forming centimeter- to decimeter-thick irregular beds, contain nondeformed larger foraminifera (alveolinids and nummulitids). Layers between these beds form seams, millimeters to centimeters thick, composed predominantly of fine-grained carbonate material, partly microcrystalline dolomite. These interlayers are locally highly microstylolitized and contain highly deformed (compressed and dissolved) *Alveolina* shells and fragmented nummulitids. These features most likely formed due to pressure solution during relatively shallow burial.

The Kozina section corresponds to the most internal part of the ramp, while the Čebulovica section in located in a more external part of the ramp (Fig. 3). The Čebulovica section is almost twice the thickness of the Kozina section. This difference is related to a combination of factors, including different positions along the ramp profile, with a higher rate of sediment accumulation in the midramp compared to the inner ramp (e.g., Pomar, 2001), different carbonate production types, with development of microbialite-coral mounds in the midramp settings (Zamagni et al., 2009), possible local differences in subsidence rates, and/or paleotopography.

Larger Benthic Foraminiferal Biostratigraphy

The biostratigraphic distributions of the index species in the studied sections were correlated using the zonation of the Paleocene and Eocene by Serra-Kiel et al. (1998), which is defined by discrete shallow benthic zones (SBZs). In the studied sections, *Glomalveolina primaeva* is restricted to SBZ3 together with the agglutinated forms *Fallotella alavensis* and *Coskinon rajkae* (Figs. 4A–4B); both taxa are restricted to the SBZ3 (Serra-Kiel at al., 1998). The base of SBZ3 is poorly constrained in our sections, mainly due to a lack of index taxa marking the SBZ2-SBZ3 boundary. In contrast, the transition from SBZ3 to SBZ4 (late Thanetian) is well defined. The precursor to SBZ4 was established by Hottinger (1960), defined by the total range of *Glomalveolina levis*. Glomalveolinids are typical of the shallow part of the ramp, which is probably the reason why they occur only in the upper part of facies association B at the shift from mid- to inner ramp deposits (within facies B7). In these shallow-water deposits, we identified *G. levis* in the Divača-Kozina West section, which appears and disappears within or at the top of SBZ4. Within SBZ4, *Assilina azilensis* and *Assilina yvettae* are common in midramp facies and represent index fossils in the study by Serra-Kiel et al. (1998) (Figs. 4C–4D). The base of SBZ5 (early Ilerdian) is easily recognized with the first appearance of true alveolinids. The total range of *Alveolina cucumiformis* (junior synonym of *Alveolina vredenburgi*; Hottinger et al., 1998) defines SBZ5. Drobne (1977) reported a reduced development of this marker species on the Adriatic carbonate platform compared to other localities in the Tethys, such as the Pyrenees. In our sections, the base of SBZ5 is marked by the first occurrences of *Alveolina aramaea aramaea* (Fig. 4F), *Alveolina avellana*, and *Alveolina globula*, all of which are restricted to SBZ5. From the SBZ5-SBZ6 limit upward, we recorded *Alveolina daniensis* (Fig. 4G), *Alveolina ellipsoidalis*, and *Alveolina pasticillata* in SBZ6; *Alveolina moussolenasis*, *Alveolina dedolia*, and *Alveolina globosa* in SBZ7; and *Alveolina corbarica* and *Alveolina brassica* in SBZ8. Other early Eocene index fossils identified together with *Alveolina* spp. are *Nummulites* spp., *Orbitolites* spp., *Opertorbitolites* spp., and *Assilina* spp., which appear within SBZ5 and above (Figs. 4H–4J).

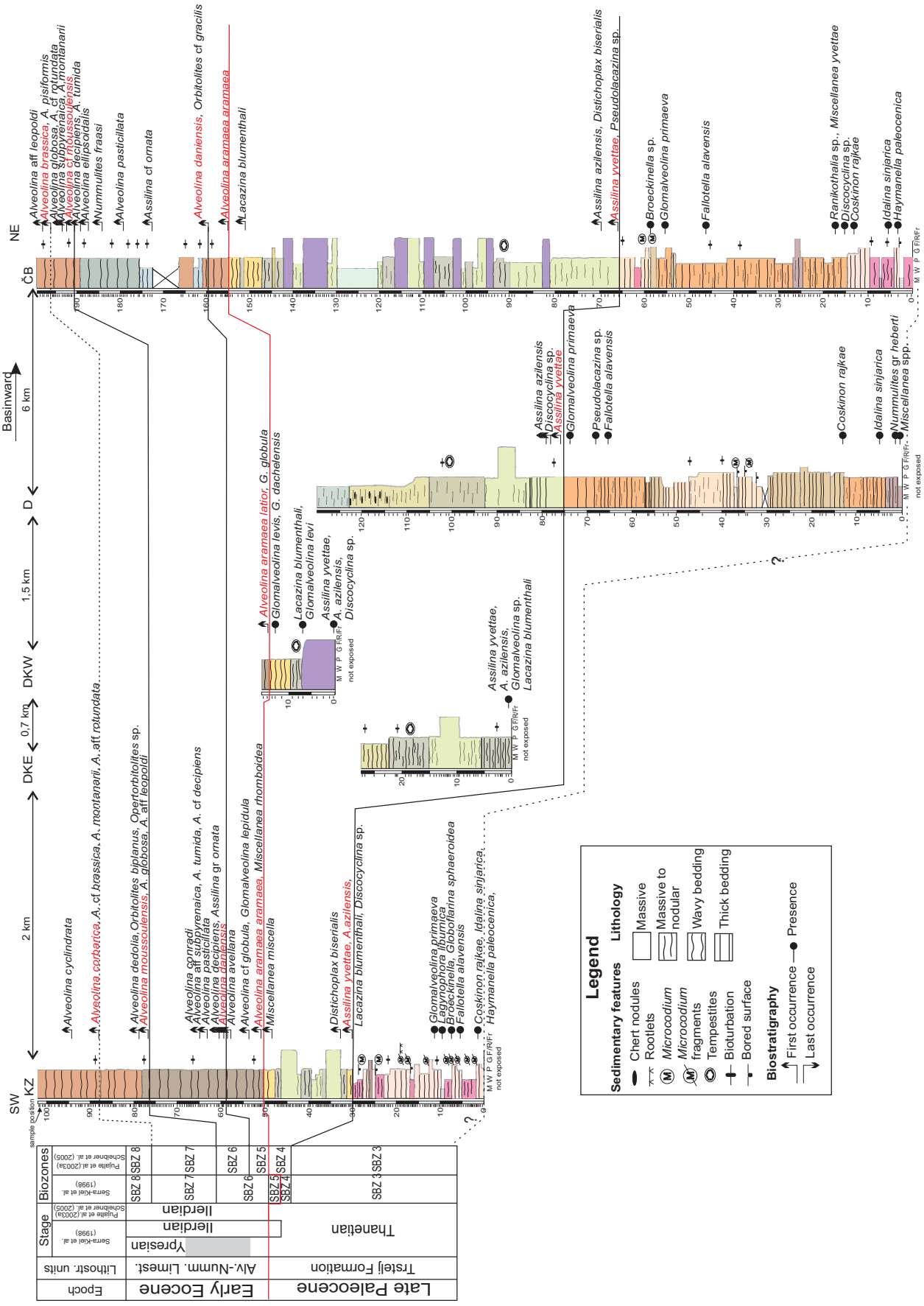

Figure 3. Stratigraphic sections and biostratigraphic markers in the studied sections, after Zamagni et al. (2008, 2009). Section labels: KZ—Kozina; ČB—Čebulovica; D—Divača; DKE—Divača-Kozina East; DKW—Divača-Kozina West. M—mudstone; W—weakstone; P—packstone; G—grainstone; F—floatstone; R—rudstone; Fr—framestone.

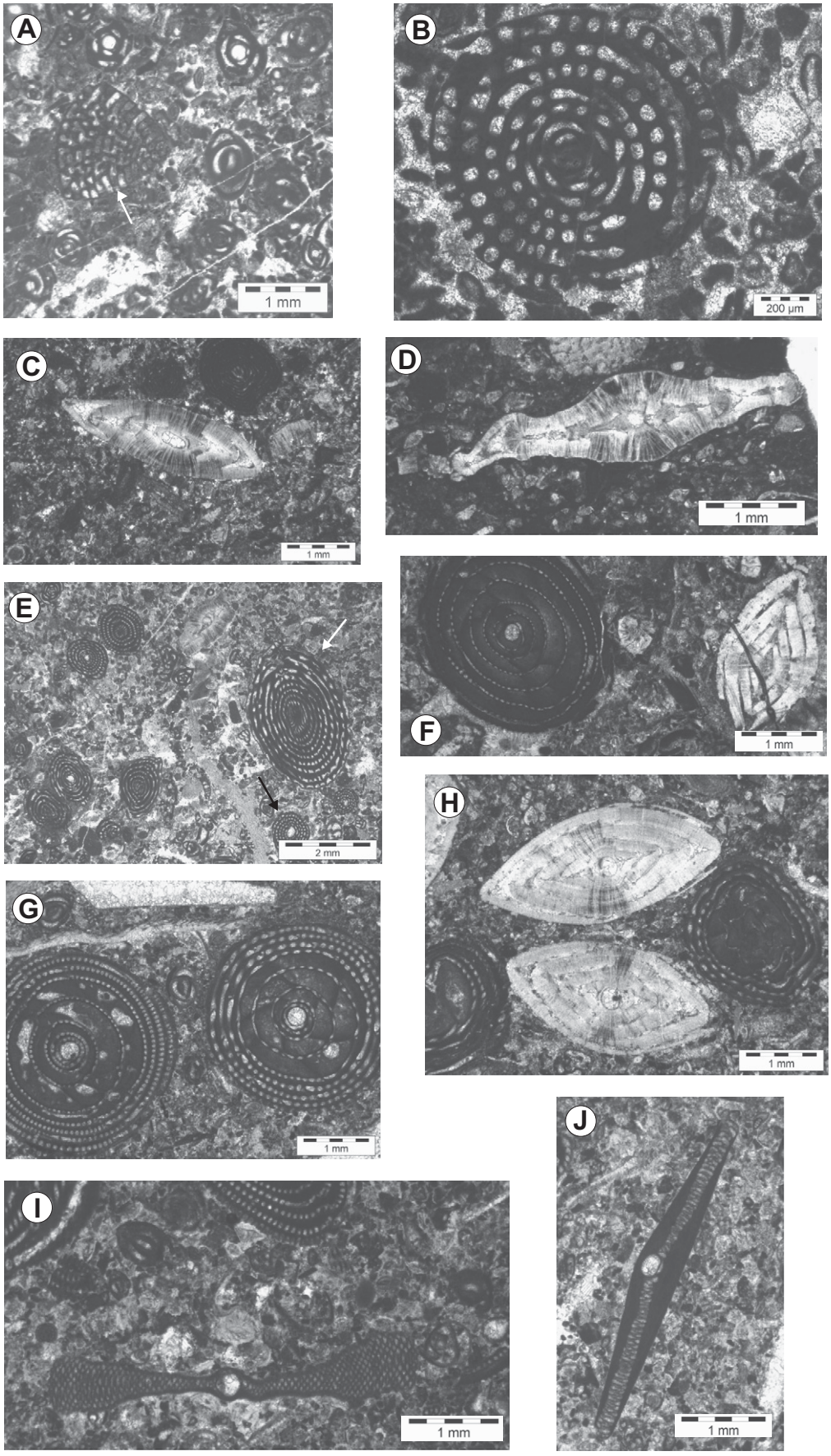

Figure 4. Larger benthic foraminifera of SBZ3–SBZ5 and SBZ6. (A) *Coskinon rajkae* (black arrow); SBZ3; sample KZ108; (B) *Glomalveolina primaeva* SBZ3; sample SI53; (C) *Assilina yvettae*; SBZ4; sample KZ149; (D) *Assilina azilensis*; SBZ4; sample SI165; (E) lacazinids (white arrow) and glomalveolinids (black arrow) SBZ4; sample KZ123; (F) *Alveolina aramaea aramaea* left side and *Nummulites* sp. right side; SBZ5; sample SI195bis; (G) *Alveolina daniensis*; SBZ6; sample SI204; (H) *Nummulites* sp. SBZ6; sample SI202; (I) *Orbitolites* sp.; SBZ6; sample KZ280; and (J) *Opertorbitolites* sp.; SBZ6; sample KZ280.

In summary, the late Paleocene can be separated into SBZ3 (early Thanetian) and SBZ4 (late Thanetian). In the studied sections, SBZ3 is characterized by the presence of *G. primaeva*, *Fallotella alavensis*, and *Coskinon rajkae* and the absence of *As. yvettae/As. azilensis*. SBZ4 is characterized mainly by the presence of *As. yvettae* and *As. azilensis*, while true alveolinids or other markers of SBZ5 are absent. SBZ5 (early Ilerdian) is characterized by first occurrences of *Alveolina* spp., together with *Nummulites* spp., *Orbitolites* sp., and *Opertorbitolites* sp.

Carbon and Oxygen Isotope Stratigraphy

The bulk-rock data are plotted against stratigraphic position and depositional facies associations in Figure 5 for the Kozina section and in Figure 6 for the Čebulovica section (see GSA Data Repository Tables DR2 and DR3 for complete isotopic data set [see footnote 1]). The Lower Thanetian (facies association A) is characterized by a large scatter in $\delta^{13}C$ values, which is more evident in the Kozina section (up to 7‰) than in the Čebulovica section (up to 3‰). The Upper Thanetian (facies association B) and the Lower Eocene (facies association C) show carbon values centered on 2‰, with an abrupt deviation at the transition between the two facies associations. A declining trend is evident in both sections in the *Glomalveolina-Assilina* packstones (facies B7), leading the onset of a negative excursion at the base of the *Alveolina* peloidal packstones (facies association C, facies C1). In the Kozina section (Fig. 5), the onset of this excursion is at 50.72 m ($\delta^{13}C$ = –0.2‰), while in the Čebulovica section (Fig. 6), the onset of the excursion occurs at 154.45 m ($\delta^{13}C$ = –2.2‰). The $\delta^{13}C$ excursions reach up to ~1‰ in the Kozina section and ~3‰ in the Čebulovica section. In both sections, the onset of the negative excursion almost coincides with the first occurrence of *Alveolina* (51.22 m in the Kozina and 155.17 m the Čebulovica). This negative excursion of $\delta^{13}C$ is maintained over a thickness of ~10 m in both sections. It is followed by isotopic values comparable to the pre-excursion values, even if slightly more positive. In the Čebulovica section, a negative $\delta^{13}C$ peak occurs before the onset of the main negative excursion, at 150.45 m ($\delta^{13}C$ = –2.0‰).

The bulk carbonate $\delta^{18}O$ measurements from the Kozina section are characterized by a wide range of values. However, a trend toward negative values can be observed throughout the Upper Paleocene, culminating with the end of the negative excursion. This first trend is followed by a trend toward more positive values in the Lower Eocene. In the Čebulovica section, a negative shift in the $\delta^{18}O$ is associated with the onset of the carbon negative excursion, followed by a wide range of values during the excursion and a trend toward more positive values in the recovery interval in the Lower Eocene.

The $\delta^{13}C$ record of large miliolids/alveolinids in the Čebulovica section (Fig. 7; GSA Data Repository Table DR4 [see footnote 1]) is characterized by a trend similar to the bulk-rock record in the Upper Thanetian, with uniform values and a negative peak at 150.45 m ($\delta^{13}C$ = –3.7‰), followed by an abrupt negative shift at 154.45 m ($\delta^{13}C$ = –7.18‰) with an excursion of ~6‰. In both bulk-rock and large miliolids/alveolinids records, the return to stable values occurs at the same point within the $\delta^{13}C$ negative excursion, and it is then maintained over a thickness of ~10 m. The nummulitid $\delta^{13}C$ record is more limited, with the first sample at 158.73 m; however, it shows a trend toward higher $\delta^{13}C$ values in correspondence with the bulk-rock excursion recovery. The matrix $\delta^{13}C$ record is characterized by a trend similar to that of large miliolids/alveolinids and bulk rock, with the negative excursion onset at 154.45 m ($\delta^{13}C$ = –4.31‰) and a decrease of ~4‰. Oxygen isotope ratios, in foraminifera and matrix records, show similar trends compared to the bulk-rock record, with a negative shift at 154.45 m concomitant with onset of the $\delta^{13}C$ excursion.

DISCUSSION

Diagenetic Effects on Carbon Isotope Curves

Diagenetic fluids, especially in meteoric environments, can modify the original stable isotope signature of shallow-marine carbonates. The most prominent carbon isotopic excursion in our data is observed in the Kozina section (~7‰) at the base of SBZ4 (Fig. 5). This interval corresponds to facies association A, representing innermost ramp depositional settings, with abundant subaerial exposure surfaces and consequently increased influence of meteoric diagenesis. This can explain the scattered patterns of oxygen and carbon values; therefore, the isotope data from this interval have been excluded from further chemostratigraphic interpretations. Up section, the successions generally exhibit gradual transitions between facies and show no abrupt change that would indicate, for example, a rapid drop of sea level. According to the well-established criteria for the recognition of subaerial exposure in the studied successions (Košir, 2004), no such surfaces have been observed in the Kozina and Čebulovica sections comprising the interval from SBZ4 (Thanetian) to SBZ8 (middle Ilerdian).

Other possible causes for deviation of original $\delta^{13}C$ values from primary signals mainly include alteration of originally unstable aragonitic material and the presence of skeletal grains that may exhibit nonequilibrium isotopic fractionation (e.g., Allan and Matthews, 1982; Joachimski, 1994; Immenhauser et al., 2002; Swart and Eberli, 2005). However, the predominant components of facies associations B and C are larger and smaller benthic foraminifera, corallinaceans and echinoderms, which were originally composed of low- to high-Mg calcite. Mineralogical stabilization of high-Mg calcite to low-Mg calcite can occur without any textural change in skeletal calcite, especially in porcelaneous foraminifera like alveolinids and larger miliolids (Budd and Hiatt, 1993). Without evidence of subvaerial exposure events, the transformation of high-Mg calcite to low-Mg calcite probably occurred under the influence of marine pore waters and had only subordinate influence on resulting C and O isotope composition of skeletal grains.

Supposedly, sediments in both sections were affected by same diagenetic history in marine and burial settings. No evidence suggests differential burial alteration at specific stratigraphic levels or facies-specific control on isotope composition.

Correlation between Biostratigraphy and Carbon Isotopic Curves

Obtaining stratigraphic controls on events recorded in shallow-water carbonates is challenging when dealing with short-lived events (10^5 yr) such as the Paleocene-Eocene thermal maximum. Starting from the late Paleocene and through the early Eocene, the diversification of larger benthic foraminifera offers the possibility to analyze high-resolution biostratigraphy in these shallow-water carbonates, due to the presence of abundant index fossils (especially alveolinids). The main problem in correlating the Paleocene-Eocene thermal maximum with the shallow benthic zones (SBZ) is the limited continuity of shallow-water marine successions containing in situ larger benthic foraminifera together with high-resolution isotopic signals recording the Paleocene-Eocene thermal maximum. There are previous reports of nearly continuous sections in the Pyrenees in which correlation between the SBZs and Paleocene-Eocene thermal maximum has been suggested (Pujalte et al., 2003a, 2009, and references therein). In these successions, the carbon isotopic excursion associated with the Paleocene-Eocene thermal maximum, however, does not seem to be fully recorded in the shallow-water marine facies, given the presence of important facies changes and the presence of nonmarine

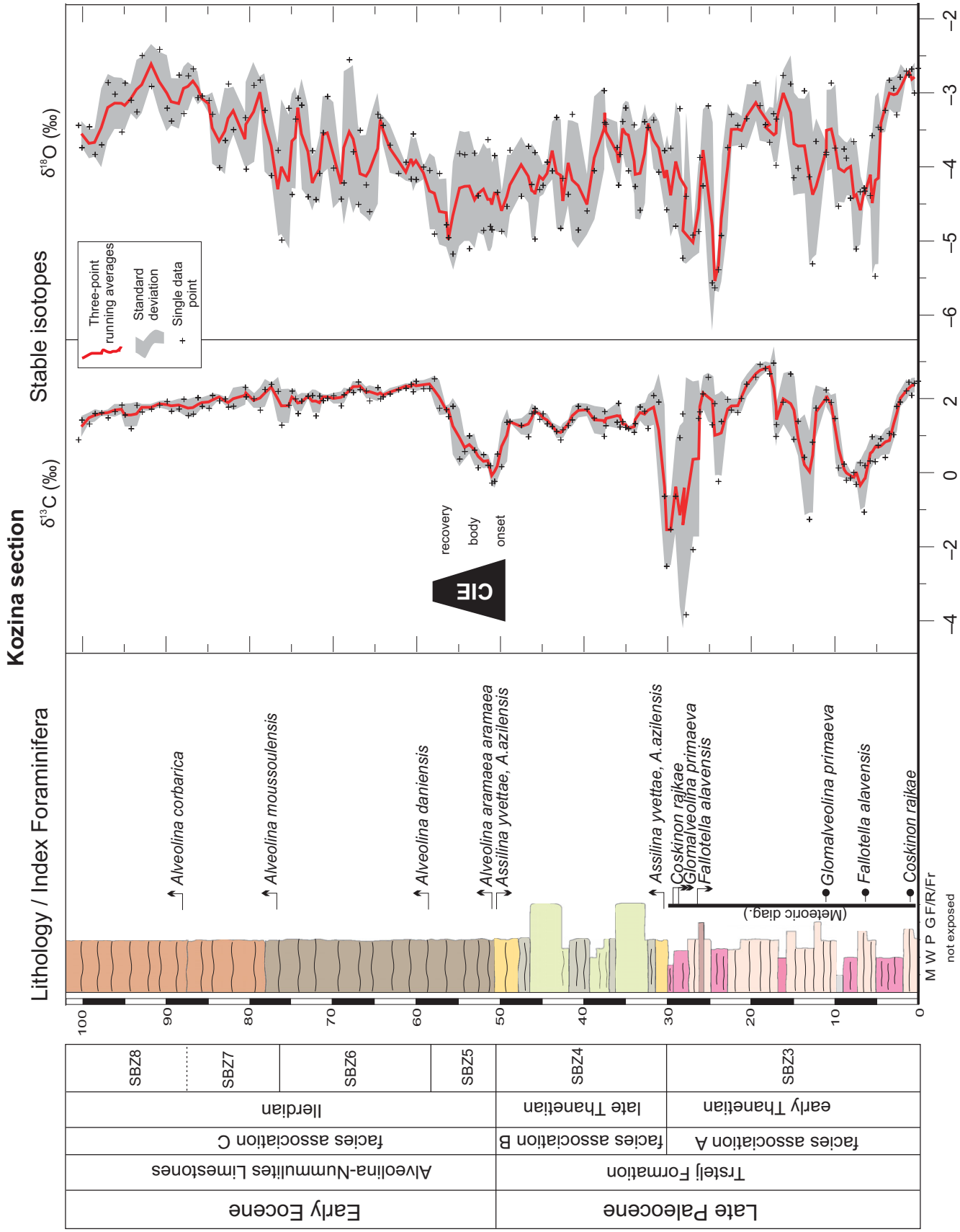

Figure 5. Biostratigraphic markers and stable isotope curves from bulk-rock samples of Kozina section. SBZ—shallow benthic zone, CIE—carbon isotopic excursion; M—mudstone; W—weakstone; P—packstone; G—grainstone; F—floatstone; R—rudstone; Fr—framestone.

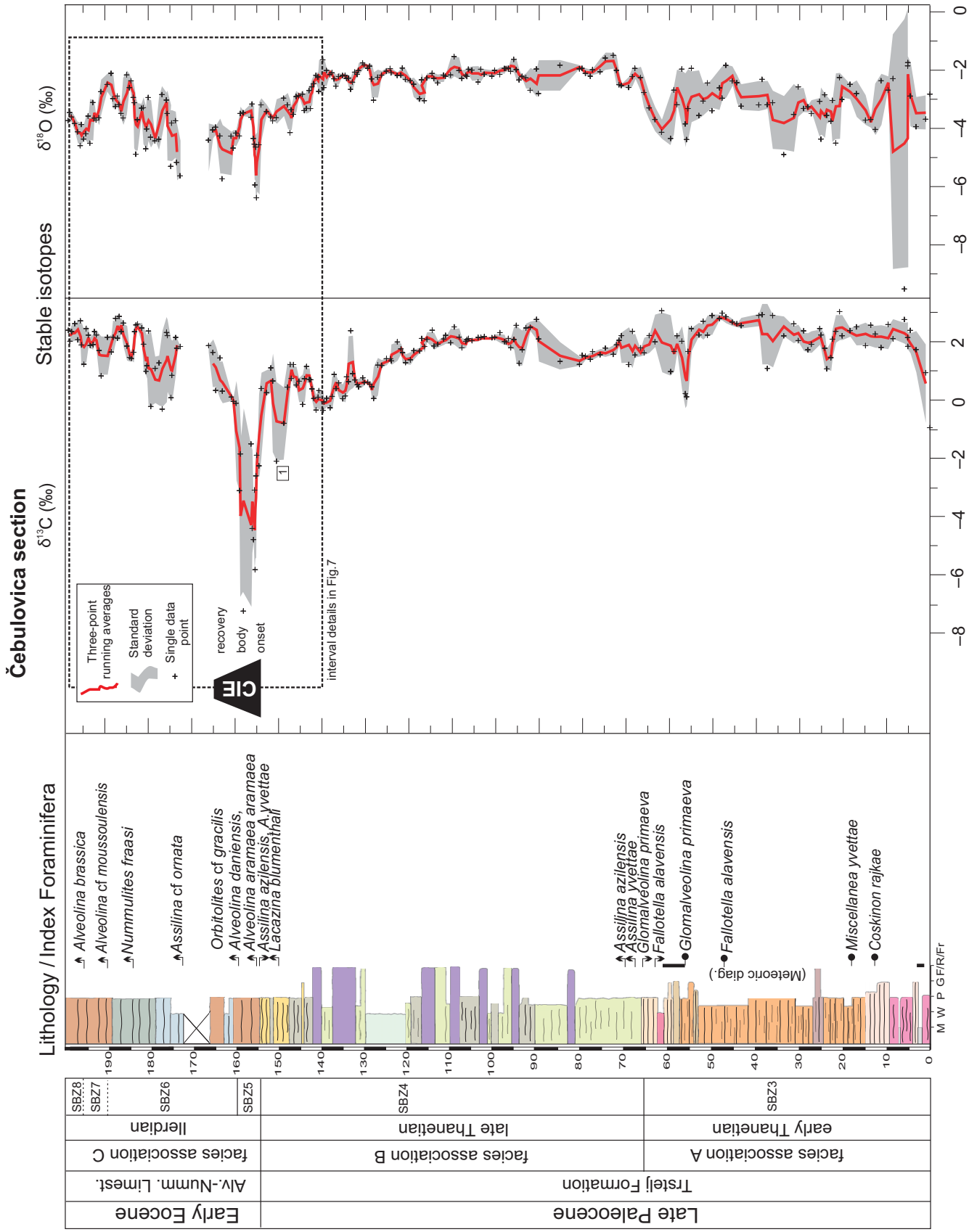

Figure 6. Biostratigraphic markers and stable isotope curves from bulk-rock samples of Čebulovica section. SBZ—shallow benthic zone, CIE—carbon isotopic excursion; M—mudstone; W—weakstone; P—packstone; G—grainstone; F—floatstone; R—rudstone; Fr—framestone.

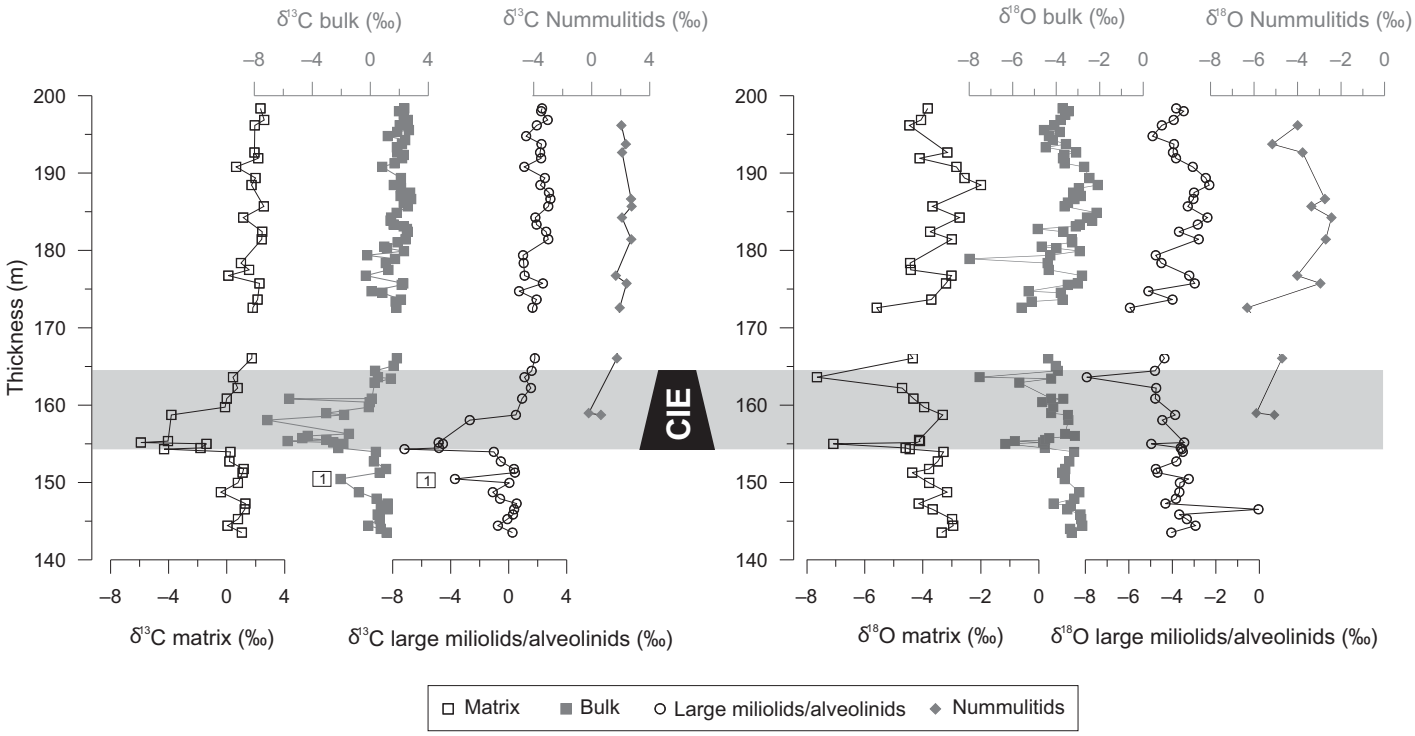

Figure 7. Isotopic curves of micrite, bulk rock, large miliolids/alveolinids, and nummulitids from Čebulovica section across the Paleocene-Eocene interval and above. Pre-execution negative spike is indicated by 1. CIE—carbon isotopic excursion.

deposits coeval with the onset of the Paleocene-Eocene thermal maximum (Campo section; Pujalte et al., 2003a, 2003b, 2009), and a regional sedimentary hiatus at the base of the Eocene (Urrobi section; Pujalte et al., 2003a).

Our studied sections apparently fulfill the requirement to combine detailed chemostratigraphy and biostratigraphy in continuous, fully marine shallow-water sections.

In both studied sections (Figs. 5–6), the onset of the most prominent negative carbon isotopic excursion coincides with the first occurrence of the early Eocene index fossil *Alveolina aramaea aramaea.* This occurrence marks the base of SBZ5 (base of the *Alveolina* peloidal packstones), while index fossils of the late Thanetian SBZ4 (*As. azilensis* and *As. yvettae*) are absent. Based on these biostratigraphic constraints, this negative carbon isotope excursion occurs at the Paleocene-Eocene boundary and thus is here interpreted as the carbon isotope excursion associated with the Paleocene-Eocene thermal maximum. The correlation between the foraminiferal biostratigraphic distributions and the isotopic signal indicates that the carbon isotopic excursion spanned SBZ5, and may have persisted through the base of SBZ6.

The use of the facies-dependent larger benthic foraminifera may be a limit for biostratigraphic purposes. In the studied sections, the level delineated as the base of the carbon isotope excursion and the Paleocene-Eocene boundary correlates with the shift from the Upper Thanetian facies B6 (*Glomalveolina-Assilina* peloidal packstone) to the Lower Eocene facies C1 (*Alveolina* peloidal packstone). This facies change, however, did not represent a significant change in terms of water depth, as demonstrated by the occurrences in the B7 facies of glomalveolinids and large miliolids (e.g., *Lacazina blumenthali*), both of which thrive in water conditions similar to those of alveolinids (Drobne and Hottinger, 2004). This observation has two main implications: (1) Any relative sea-level changes in the studied area were minor, despite other studies that have suggested sea-level rise at this time (e.g., Sluijs and Brinkhuis, 2009); and (2) the occurrence of the lowermost *Alveolina* in our sections represents a true occurrence rather than a facies-dependent occurrence.

In summary, in both study sections, the onset of the carbon isotopic excursion coincides with the lowest occurrence of the marker species for SBZ5. Because the base of the carbon isotopic excursion delineates the Paleocene-Eocene boundary (Aubry et al., 2007), these results demonstrate a clear correlation between the Paleocene-Eocene boundary and the SBZ4-SBZ5 boundary in the shallow benthic zonation of Serra-Kiel et al. (1998). This pattern is consistent with the records from the Pyrenees (Orue-Etxebarria et al., 2001; Pujalte et al., 2003a, 2009) and Egypt (Scheibner et al., 2005; Scheibner and Speijer, 2009), further emphasizing the necessity for a revision of the chronostratigraphy of the early Eocene, with the bases of both the global Ypresian Stage (Gradstein et al., 2004) and the regional Ilerdian Stage (redefined by Pujalte et al., 2009) considered coeval.

Comparison between Paleocene-Eocene Thermal Maximum in the Shallow-Water Successions of the Adriatic Carbonate Platform and Other Marine Paleocene-Eocene Thermal Maximum Records

Geologically brief episodes of perturbation of the carbon cycle (carbon isotopic excursions) associated with rapid climate changes have occurred frequently throughout Earth history (for a revision of the main carbon isotopic excursions during the Mesozoic and a comparison with the Paleocene-Eocene thermal maximum, see, e.g., Jenkyns, 2003, and references therein). There is, however, a lack of isotopic studies for the Paleocene-Eocene thermal maximum on shallow-water carbonates similar to the one presented in our study, which has hindered an assessment of the magnitude and shape of the carbon isotope

excursion. The amplitude of the carbon isotope excursion on bulk-rock records (~1‰ in section Kozina and ~3‰ in Čebulovica; Figs. 5 and 6) is comparable to values reported in the literature for shallow-marine continental margins (e.g., between 2.8‰ and 3.5‰ for the North American shelf; John et al., 2008), Pacific guyot (~3‰; Robinson, 2011), and deep-sea bulk carbonates (between 2.5‰ and 4.0‰). The onset of the carbon isotope excursion in both sections is gradual, especially in the Kozina section, with the most negative values occurring during the main body of the excursion. This is not the case in the foraminiferal record (Fig. 7), but this may be related to the reduced number of samples. The gradual carbon isotope excursion onset in our bulk-rock records contrasts with a more abrupt onset from the North American shelves and pelagic $\delta^{13}C$ records, where dissolution might have played some role (Zachos et al., 2005; John et al., 2008). The gradual onset combined with the apparent continuity in sedimentation suggest that the carbon isotope excursion in our sections may have been fully recorded.

The carbon isotope ratios of our shallow-marine carbonates from the Čebulovica section are strongly ^{13}C-depleted compared to open-marine records of the Paleocene-Eocene thermal maximum, with excursion bulk-rock values up to –7‰ and matrix $\delta^{13}C$ up to –5.9‰ (Figs. 6–7). The bulk-rock values of shallow-water carbonates can be the result of combined effects of different processes; hence, they must be considered carefully. Shallow, neritic water masses and their carbon cycles are commonly decoupled from those of deep epicontinental basins and the open ocean (Immenhauser et al., 2008, and references therein). Modern carbonate platform settings such as Florida Bay and the Bahamas (Patterson and Walter, 1994b) and fossil examples (Immenhauser et al., 2008) show proximal-distal gradients in their $\delta^{13}C$ records of dissolved inorganic carbon (DIC), with decreased $\delta^{13}C$ values for the inner platform compared to adjacent open ocean. In all these examples, the intraplatform gradients in the $\delta^{13}C$ record were inferred to result from a complex interaction of sedimentological, physico-chemical, and biological processes. In particular, the low $\delta^{13}C$ inner platform data have been related to: (1) restriction and smaller carbon reservoir size of the platform–top water mass; (2) the influence of the local carbon weathering fluxes from the land; or (3) syndepositional diagenesis of carbonate mud in organic-rich sediments (Immenhauser et al., 2008). The relative contribution of each of these processes, however, is difficult to quantify, even in modern environments (Patterson and Walter, 1994a, 1994b). In the case of the Adriatic carbonate platform, the deposition of the studied sections occurred in a ramp setting, probably characterized by strong current activity (Zamagni et al., 2008, 2009). Wave- and current-driven exchange between the open sea and the shallow, neritic sea likely limited the restriction of the water masses. Oxidation and respiration of organic matter would have resulted in ^{13}C-depleted pore-water values (Sanders, 2003, and reference therein). Syndepositional dissolution of $CaCO_3$ due to organic matter oxidation affects the original carbonate sediment $\delta^{13}C$ values and imparts low $\delta^{13}C$ values to syndepositional diagenetic carbonate (Sanders, 2003; Patterson and Walter, 1994a). The strongly ^{13}C-depleted values of the studied shallow-marine carbonates might, therefore, partly represent syndepositional alteration of organic matter. The record of the Paleocene-Eocene thermal maximum is consistent with such interpretation, with intensified chemical weathering and river runoff (e.g., Egger et al., 2005; Giusberti et al., 2007), increased seasonality, especially at intermediate latitudes, inducing more efficient physical weathering and erosion (Schmitz and Pujalte, 2003, 2007), and accumulation of organic-rich deposits and black shale deposits along the margin of the Tethys (Bolle and Adatte, 2001; Speijer and Wagner, 2002; Gavrilov et al., 2003). The differences in the $\delta^{13}C$ values during the Paleocene-Eocene thermal maximum between the Kozina and the Čebulovica sections, with the former characterized by less negative excursion $\delta^{13}C$ values, might be related to current-driven redistribution of the organic matter along the carbonate ramp. The spatial extent of the study area is too small to explain this diversity with different organic matter type or preservation along the depositional area (Hedges and Keil, 1995).

The $\delta^{13}C$ excursion in the large miliolid/alveolinid record from the Čebulovica section is ~6‰. No similar records for large benthic foraminifera have been published so far. The most similar $\delta^{13}C$ foraminifera record is based on planktonic foraminifera from the Wilson Lake section (the mixed layer dweller *Acarinina*; Zachos et al., 2006), which shows an ~4‰ excursion. Low $\delta^{13}C$ values recorded in the large miliolids/alveolinids (up to –7.18‰) might be related to the presence of symbionts, which could have promoted isotopic fractionation. Studies of the isotopic composition of Recent symbiont-bearing foraminifera (e.g., Langer, 1995), however, show consistently higher $\delta^{13}C$ values in miliolid foraminifers (e.g., $\delta^{13}C$ values for *Alveolinella quoyii* ranging between 1.9‰ and 2.5‰) compared with rotaliids as a result of metabolic processes and/or biomineralization overprints acting as isotopic filters. These results suggest exclusion of important "vital effects" affecting the isotopic values of big miliolids/alveolinids from the studied sections. Assuming that the foraminifera shells were not affected by early marine or meteoric diagenesis, the foraminiferal carbon isotope values, which are comparable to the bulk-rock values, might indicate that there was a true lowering of seawater $\delta^{13}C$ values in the shallow waters related to depositional conditions during the Paleocene-Eocene thermal maximum. This hypothesis, however, deserves further study, in order to get a better picture of the impact of the Paleocene-Eocene thermal maximum event on the carbon cycle of the shallow-water realm.

The carbon isotope excursion in the matrix micrite of the Čebulovica section is ~4‰, an intermediate value compared to bulk-rock and foraminifera data. This excursion value falls between the 2.8‰–3.5‰ of the continental shelves and the ~5‰–6‰ of the terrestrial records in soil carbonate nodules (e.g., Bowen et al., 2001) and total organic carbon (Magioncalda et al., 2004). Several studies have demonstrated that the carbonate matrix micrite $\delta^{13}C$ time-series data are, under favorable conditions, a reasonable qualitative proxy for first-order chemostratigraphic trends in past $\delta^{13}C$ seawater (e.g., Weissert et al., 1985; Immenhauser et al., 2002, 2008).

Interestingly, in both bulk-rock and foraminifera $\delta^{13}C$ curves of the Čebulovica section, a negative spike has been detected prior to the full onset of the carbon isotope excursion (indicated as 1 in Figs. 6–7). Similar negative spikes preceding the main carbon isotope excursion have also been identified in other studies, especially in terrestrial records (e.g., Magioncalda et al., 2004; Domingo et al., 2009), while in marine records, it is only vaguely recognizable (e.g., bulk-rock data from Tumey Gulch section, California—John et al., 2008; benthic foraminifera records from Wilson Lake section—Zachos et al., 2006). Although it is recorded with only one data point, this spike may represent a perturbation of the carbon exogenic pool prior to the main perturbation related to the Paleocene-Eocene thermal maximum.

Larger Benthic Foraminiferal Evolution and the Paleocene-Eocene Thermal Maximum

Larger benthic foraminifera are characterized by a symbiotic relationship with algae, large size, and adult dimorphism (Hottinger, 1982). These properties allow them to thrive under seasonal changes in warm, oligotrophic environments, where algal symbiosis offers great advantages (Hottinger, 1983; Hallock, 1985). The evolution of larger benthic foraminifera

during the early Paleogene was primarily a long-term process of reorganization of the group after the Cretaceous-Tertiary crisis (Hottinger, 1998). A rapid diversification of species belonging to a restricted number of successful genera (mainly alveolinids and nummulitids) close to the Paleocene-Eocene boundary was first described from the Pyrenees by Hottinger and Schaub (1960). This biotic event marks the base of the Ilerdian, placed between SBZ4 and SBZ5 (Hottinger and Schaub, 1960; Hottinger, 1998). A causal link between the Paleocene-Eocene thermal maximum and this turnover in the larger benthic foraminifera communities has been suggested (Orue-Etxebarria et al., 2001; Pujalte et al., 2003a, 2003b, 2009; Scheibner et al., 2005; Scheibner and Speijer, 2009). An accurate correlation between the carbon isotopic excursion and the evolution of the larger benthic foraminifera, however, has remained elusive.

The high-resolution correlation presented in this study between the foraminiferal biostratigraphic distributions and the carbon isotope excursion allows for a detailed documentation of the timing and nature of the larger foraminifera turnover. Based on our correlation, the turnover occurred through a two-step process (Fig. 8). The first step is marked by an initial, rapid diversification of small alveolinids and nummulitids during the SBZ5 and SBZ6 (early Ilerdian) interval, followed by a second step starting from SBZ7 (middle Ilerdian) that is characterized by further specific diversification, increase of shell size, and well-developed adult dimorphism. The first step was coeval with the onset of the carbon isotope excursion, whereas the second step took place well after the end of the Paleocene-Eocene thermal maximum event. Did external environmental forcing such as the rapid temperature increase and heat stress associated with the Paleocene-Eocene thermal maximum exert direct effects in shaping the larger benthic foraminifera assemblage compositions? The progressive increase in shell size and development of adult dimorphism are typical features of long-term maturation cycles within larger benthic foraminifera communities (Hottinger, 1998). Within an evolutionary scheme mainly controlled by the development of the Eocene global community maturation cycle (Hottinger, 1998), we argue that high seawater temperatures recorded during the Paleocene-Eocene thermal maximum (up to 35 °C at midlatitudes; Zachos et al. 2006) could have stimulated the rapid specific diversification that characterizes the first step of the turnover during the early Ilerdian. Larger benthic foraminifera are ectotherm organisms, with body temperatures tending to equilibrate with ambient temperatures. Because the kinetics of chemical reactions associated with metabolism are a function of temperature (Hallock et al., 1991), increased temperatures would have a major effect on foraminiferal life processes. Recent studies, for example, have demonstrated that diversity is directly correlated with speciation rate and that both phenomena seem to be causally linked to increased temperature (Escarguel et al., 2008). Increase in phenotypic diversification has also been linked to acceleration of mutation rates due to repairs of deoxyribonucleic acid (DNA) damaged by extreme environmental conditions, such as increases in ultraviolet (UV)-B radiation (e.g., morphological variability in Recent *Amphistegina* offspring; Hallock, 2000).

Even if the effects of sea-surface temperature changes on Recent larger benthic foraminifera are well constrained (Langer and Hottinger, 2000), the range of nutrient concentrations under which they can thrive is poorly defined (Hottinger, 1983). Many studies have highlighted a major increase in the hydrological cycle and chemical weathering during the Paleocene-Eocene thermal maximum (e.g., Pagani et al., 2006; Ravizza et al., 2001; Egger et al., 2005), with enhanced runoff, stratification, and eutrophic conditions in coastal waters (e.g., Bujak and Brinkhuis, 1998; Crouch et al., 2003; Egger et al., 2003, 2005; Gibbs et al., 2006). It has been suggested that the climate at midlatitudes became more seasonally extreme at this time, with brief, intense wet seasons and prolonged dry seasons (Egger et al., 2005; Schmitz and Pujalte, 2003, 2007). Within this framework, the appearance and spread of *Alveolina* and *Nummulites* (both taxa considered to be adapted to live in low-nutrient, stable environments; Hottinger, 1983) at the Paleocene-Eocene boundary concomitant with the thermal maximum suggest that either (1) the shallow waters were not significantly affected by increased nutrients; or (2) the early Ilerdian (SBZ5–SBZ6) larger benthic foraminifera were highly resilient and adapted to exploit the enhanced nutrient levels without adverse effects. A combination of both conditions is most likely given that: (1) carbonate ramps, which were common during the early Paleogene in the Tethys (Buxton and Pedley, 1989), are characterized by strong current activity and redistribution of sediment (Pomar, 2001), which would have limited concentration of the nutrients and consequent development of eutrophic, anoxic conditions; and (2) the early Ilerdian alveolinids and nummulitids have relatively small dimensions, with diameters less than 4 mm and a weak adult dimorphism compared to their counterparts that evolved afterward (second step during the middle Ilerdian; Fig. 8), suggesting the ability to acclimatize to relatively high or frequently fluctuating nutrient levels. Thus, our correlation between the Paleocene-Eocene thermal maximum and the evolution of larger benthic foraminifera suggests that changes in the nutrient cycle (even if no extreme eutrophication has been observed in this region), and high sea-surface temperatures likely induced some adaptations in the larger benthic foraminifera community, influencing the larger benthic foraminifera turnover.

Ocean Acidification during the Paleocene-Eocene Thermal Maximum: An Overview from the Shallow-Water Realm

The geologically rapid increase in pCO_2 during the Paleocene-Eocene thermal maximum would have significantly affected seawater pH, leading to varying degrees of decreased carbonate saturation in the deep-sea ocean (e.g., Zachos et al., 2005, 2008; Ridgwell and Schmidt, 2010) and producing a phenomenon known as "ocean acidification" (i.e., Caldeira and Wickett, 2003; Kump et al., 2009; Doney et al., 2009). Clay or low-carbonate layers coincident with the Paleocene-Eocene thermal maximum have been identified in several deep-sea cores and land-based marine sections interpreted as resulting from deep-sea undersaturation with respect to calcite (e.g., Zachos et al., 2005; Giusberti et al., 2007; Alegret et al., 2009). The extinction of deep-sea benthic foraminifera concomitant with the Paleocene-Eocene thermal maximum, particularly affecting calcifying forms, has been well documented (e.g., Thomas, 1998) and interpreted as a combination of calcite undersaturation, basinal anoxia, and increased temperatures (e.g., Thomas, 2007). Conversely, studies on pelagic marine calcifiers concluded that there is little evidence for detrimental effects resulting directly from surface-water acidification during the Paleocene-Eocene thermal maximum (Gibbs et al., 2006, 2010).

The responses of shallow-water carbonate ecosystems to changes in surface ocean chemistry during the Paleocene-Eocene thermal maximum have received less attention (Robinson, 2011). In our studied sections, the thickness of the carbon isotopic excursion associated with the Paleocene-Eocene thermal maximum is ~10 m, and our sampling density was up to 5 samples/m. Because we do not observe significant facies changes pointing to deepening or shallowing trends for this interval, we can assume a fairly constant sediment accumulation rate. Thus, the probability of recording any short period (~10^4 yr) of significant change in the surface-ocean chemistry (mainly decreases in surface ocean pH) is relatively good. Our larger benthic foraminifera do not show clear evidence of morphological abnormalities (e.g.,

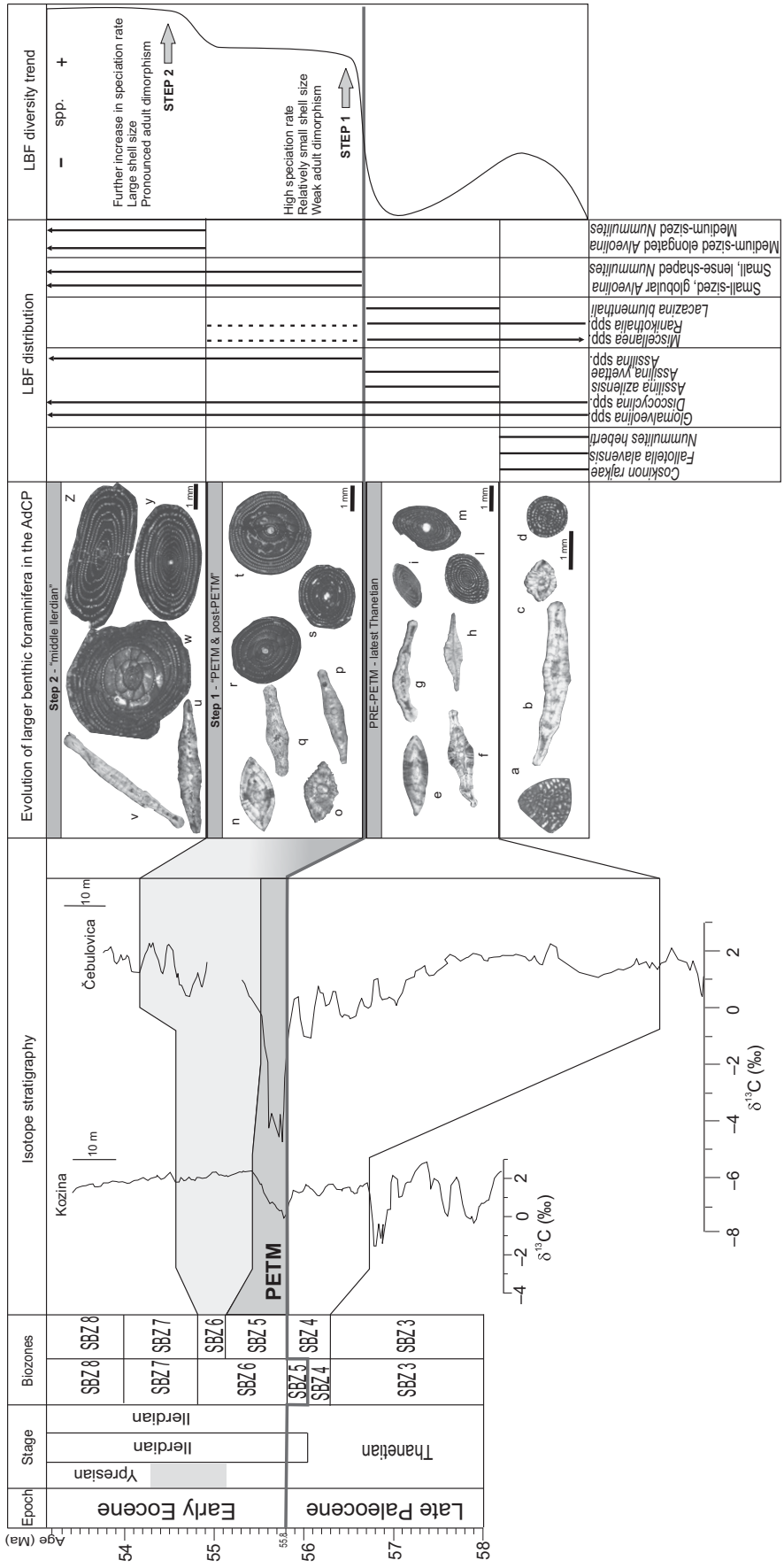

Figure 8. Correlation between $\delta^{13}C$ curves and the biostratigraphic distributions of larger benthic foraminifera (LBF). The $\delta^{13}C$ bulk record from the late Paleocene to the early Eocene, through the carbon isotope excursion (CIE), at Čebulovica and Kozina sections is correlated with the biostratigraphic distributions of the larger benthic foraminifera and their evolution in terms of size increase. The $\delta^{13}C$ curve of the Čebulovica section is not complete and starts from 55 m. Biostratigraphic distribution of larger benthic foraminifera is based on their occurrences in the studied sections (continuous line) and literature (dashed line). Larger benthic foraminifera specific diversity trend is after Hottinger (1998) and Orue-Etxebarria et al. (2001). Larger benthic foraminifera from the Adriatic carbonate platform (AdCP) sections: (a) *Coskinon rajkae*; (b) *Nummulites* cf. *heberti*; (c) *Miscellanea yvettae*; (d) *Glomalveolina primaeva*; (e) *Assilina yvettae*; (f) *Assilina aziensis*; (g) *Ranikothalia* sp.; (h) *Discocyclina seunesi*; (i) *Glomalveolina levis*; (l) *Glomalveolina* sp.; (m) *Lacazina blumenthali*; (n) *Nummulites* sp.; (o) *Miscellanea rhomboidea*; (p) *Nummulites* cf. *fraasi*; (q) *Ranikothalia* sp.; (r) *Alveolina aramaea aramaea*; (s) *Alveolina avellana*; (t) *Alveolina daniensis*; (u) *Assilina* cf. *ornata*; (v) *Ranikothalia* sp.; (w) *Alveolina montanarii*; (y) *Alveolina moussoulensis*; (z) *Alveolina* cf. *rotundata*. Note change of scale from the association of SBZ3 to that of SBZ4. PETM—Paleocene-Eocene thermal maximum; SBZ–shallow benthic zone.

brakeage and repair or distorted shells) that might suggest problems during biocalcification processes (Toler and Hallock, 1998). Either the carbon release during the Paleocene-Eocene thermal maximum was too slow to significantly acidify surface water (e.g., Zachos et al., 2008; Ridgwell and Schmidt, 2010), or larger benthic foraminifera were relatively insensitive to variations in pH. Others organisms, especially aragonitic scleractinian corals, might have been more severely affected by changes in surface seawater pH during the Paleocene-Eocene thermal maximum, resulting in reduction of calcification rates (Zamagni et al., 2012) and reef accretion (e.g., Kiessling and Simpson, 2011). Further studies, however, are necessary to add useful information to the debate about whether there was a significant acidification affecting shallow-water settings during the Paleocene-Eocene thermal maximum.

CONCLUSIONS

The combination of larger benthic foraminiferal biostratigraphy with carbon and oxygen isotope stratigraphy of the sedimentary successions on the Adriatic carbonate platform in SW Slovenia allowed us to conduct a high-resolution exploration of the Paleocene-Eocene thermal maximum in shallow-marine carbonates. Our data document in detail the carbon isotopic excursion related to the Paleocene-Eocene thermal maximum in continuous, fully marine shallow-water carbonates. The onset of the excursion occurs at the base of the *Alveolina* limestones, confirming that the Paleocene-Eocene limit should be correlated with the SBZ4-SBZ5 boundary, and so the base of the Ypresian should coincide with the base of the Ilerdian. The carbon isotopic excursion is expressed by a negative excursion of ~1‰ in the bulk-rock samples of the proximal Kozina section and ~3‰ in the distal Čebulovica section within a stratigraphic interval where no evidence of sedimentary hiatuses has been observed. The $\delta^{13}C$ excursion is recorded by the different rock components of the Čebulovica section and varies between ~6‰ (large miliolids/alveolinids) and ~4‰ (matrix micrite). Syndepositional dissolution of $CaCO_3$ due to organic matter oxidation might have produced the strongly ^{13}C-depleted values of the studied shallow-marine carbonates compared to open-marine $\delta^{13}C$ excursion values. Increase of organic matter delivery could be explained by intensified weathering and river runoff during the Paleocene-Eocene thermal maximum. The differences in excursion $\delta^{13}C$ values between the two studied sections may be the result of depositional conditions with current-induced redistribution of organic matter along the ramp. Further detailed studies are, however, necessary to test this hypothesis, in order to better characterize the impact of the Paleocene-Eocene thermal maximum event on the carbon cycle of the shallow-water realm. Nonetheless, these data confirm the strong potential of shallow-water carbonates from the Adriatic carbonate platform to serve as a paleoclimatic archive, as they so far represent the most complete successions across the Paleocene-Eocene limit with a detailed record of the short-lived carbon isotopic excursion event associated with the Paleocene-Eocene thermal maximum.

The correlation between the continuous succession of larger benthic foraminifera and the carbon isotopic excursion in the shallow-marine carbonates of our study sections provides a detailed documentation of the nature and timing of the Ilerdian larger foraminifera turnover. We describe a two-step process, with a first step (early Ilerdian SBZ5-SBZ6) coinciding with the onset of the carbon isotopic excursion, characterized by a rapid specific diversification of relatively small alveolinids and nummulitids, and a second step (middle Ilerdian SBZ7) occurring well after the end of the Paleocene-Eocene thermal maximum event, characterized by a further increase of shell size, speciation rate, and development of adult dimorphism. We argue that within an evolutionary history largely driven by the long-term Eocene global community maturation cycle, the high sea-surface temperatures associated with the Paleocene-Eocene thermal maximum might have promoted the speciation rate of larger foraminifera during the earliest Ilerdian. Additionally, fluctuating nutrient levels due to enhanced runoff during the Paleocene-Eocene thermal maximum might have induced some provisional morphological adaptations in the early Ilerdian larger foraminifera (relatively small shell size, weak adult dimorphism). Finally, no evidence for problems in production of biogenic carbonate (biocalcification crisis) affecting larger benthic foraminifera has been observed. We argue, therefore, that the effects of any changes in surface ocean pH during the Paleocene-Eocene thermal maximum were minor.

ACKNOWLEDGMENTS

We thank the German Science Foundation (DFG project MU1680/7-1), the International Association of Sedimentologists, and the Graduate School of the University of Potsdam for the grants awarded to Jessica Zamagni. We are grateful to Helmut Weissert and Cédric M. John for their help and fruitful discussions. We thank Christine Fischer for preparation of thin sections. Tom Benson is gratefully acknowledged for help with the microdrilling of samples. We are grateful to Birgit Plessen (GFZ, Potsdam) and Stefano Bernasconi (ETH Zürich) for laboratory assistance with stable isotope analyses. Taylor F. Schildgen is thanked for valuable improvement of the English. We especially appreciate the many valuable suggestions and constructive comments made by reviewers Adrian Immenhauser and Victoriano Pujalte, as well as Associate Editor Brian Pratt, which greatly improved the manuscript. This work is dedicated to Lukas Hottinger. In particular, Jessica is grateful to him and his family for having opened the doors of their home during three unforgettable days.

REFERENCES CITED

Alegret, L., Ortiz, S., Orue-Etxebarria, X., Bernaola, G., Baceta, J.I., Monechi, S., Apellaniz, E., and Pujalte, V., 2009, The Paleocene-Eocene Thermal Maximum: new data from the microfossil turnover at the Zumaia section, Spain: Palaios, v. 24, p. 318–328.

Allan, J.R., and Matthews, R.K., 1982, Isotope signature associated with early meteoric diagenesis: Sedimentology, v. 29, p. 797–817, doi:10.1111/j.1365-3091.1982.tb00085.x.

Aubry, M.P., Ouda, K., Dupuis, C., Berggren, W.A., Van Couvering, J.A., and the Members of the Working Group on the Paleocene/Eocene Boundary, 2007, The global standard stratotype-section and point (GSSP) for the base of the Eocene Series in the Dababiya section (Egypt): Episodes, v. 30, no. 4, p. 271–286.

Bains, S., Corfield, R.M., and Norris, R.D., 1999, Mechanisms of climate warming at the end of the Paleocene: Science, v. 285, p. 724–727, doi:10.1126/science.285.5428.724.

Bolle, M.-P., and Adatte, T., 2001, Paleocene–early Eocene climatic evolution in the Tethyan realm: Clay mineral evidence: Clay Minerals, v. 36, p. 249–261, doi:10.1180/000985501750177979.

Bowen, G.J., Koch, P.K., Gingerich, P.D., Norris, R.D., Bains, S., and Corfield, R.M., 2001, Refined isotope stratigraphy across the continental Paleocene-Eocene boundary on Polecat Bench in the northern Bighorn Basin, *in* Gingerich, P.D., ed., Paleocene-Eocene Stratigraphy and Biotic Change in the Bighorn and Clarks Fork Basins, Wyoming: University of Michigan Papers on Paleontology 33, p. 73–88.

Budd, A.D., and Hiatt, E.E., 1993, Mineralogical stabilization of high-magnesium calcite—Geochemical evidence for intracrystal recrystallization within Holocene porcellaneous foraminifera: Journal of Sedimentary Petrology, v. 63, p. 261–274.

Bujak, J.P., and Brinkhuis, H., 1998, Global warming and dinocyst changes across the Paleocene/Eocene Epoch boundary, *in* Aubry, M.-P., Lucas, S.G., and Berggren, W.A., eds., Late Paleocene–Early Eocene Biotic and Climatic Events in the Marine and Terrestrial Records: New York, Columbia University Press, p. 277–295.

Buxton, M.W.N., and Pedley, H.M., 1989, Short paper: A standardized model for Tethyan Tertiary carbonate ramps: Journal of the Geological Society of London, v. 146, p. 746–748, doi:10.1144/gsjgs.146.5.0746.

Caldeira, K., and Wickett, M.E., 2003, Anthropogenic carbon and ocean pH: Nature, v. 425, p. 365–368, doi:10.1038/425365a.

Crouch, E.M., Heilmann-Clausen, C., Brinkhuis, H., Morgans, H.E.G., Rogers, K.M., Egger, H., and Schmitz, B., 2001, Global dinoflagellate event associated with the late Paleocene thermal maximum: Geology, v. 29, p. 315–318, doi:10.1130/0091-7613(2001)029<0315:GDEAWT>2.0.CO;2.

Crouch, E.M., Brinkhuis, H., Visscher, H., Adatte, T., and Bolle, M.-P., 2003, Late Paleocene–early Eocene dinoflagellate cyst records from the Tethys: Further observations on the global distribution of *Apectodinium*, *in* Wing, S.L., Gingerich, P.D., Schmitz, B., and Thomas, E., eds., Causes and Consequences of Globally Warm Climates in the Early Paleogene: Geological Society of America Special Paper 369, p. 113–131.

Dickens, G.R., O'Neil, J.R., Rea, D.K., and Owen, R.M., 1995, Dissociation of oceanic methane hydrate as a cause of the carbon isotope excursion at the end of the Paleocene: Paleoceanography, v. 10, p. 965–971, doi:10.1029/95PA02087.

Dickens, G.R., Castillo, M.M., and Walker, J.C.G., 1997, A blast of gas in the latest Paleocene: Simulating first-

order effects of massive dissociation of oceanic methane hydrate: Geology, v. 25, p. 259–262, doi:10.1130/0091-7613(1997)025<0259:ABOGIT>2.3.CO;2.

Domingo, L., López-Martínez, N., Leng, M.J., and Grimes, S.T., 2009, The Paleocene–Eocene thermal maximum record in the organic matter of the Claret and Tendruy continental sections (south-central Pyrenees, Lleida, Spain): Earth and Planetary Science Letters, v. 281, p. 226–237, doi:10.1016/j.epsl.2009.02.025.

Doney, S.C., Balch, W.M., Fabry, V.J., and Feely, R.A., 2009, Ocean acidification, a critical emerging problem for the ocean sciences: Oceanography (Washington, D.C.), v. 22, p. 16–25, doi:10.5670/oceanog.2009.93.

Drobne, K., 1977, Alveolines Paleogenes de la Slovenie et de l'Istrie: Mémoires Suisses de Paléontologie 99, Birkhäuser (Basel), 132 p.

Drobne, K., and Hottinger, L., 2004, Larger miliolid foraminifers in time and space. Académie Serbe des Sciences et des Arts, Bulletin T. CXXVIII: Sciences Naturelles, v. 42, p. 83–99.

Egger, H., Fenner, J., Heilmann-Clausen, C., Rögl, F., Sachsenhofer, R., and Schmitz, B., 2003, Paleoproductivity of the northwestern Tethyan margin (Anthering section, Austria) across the Paleocene-Eocene transition, *in* Wing, S.L., Gingerich, P.D., Schmitz, B., and Thomas, E., eds., Causes and Consequences of Globally Warm Climates in the Early Paleogene: Geological Society of America Special Paper 369, p. 133–146.

Egger, H., Homayouna, M., Huber, H., Rögl, F., and Schmitz, B., 2005, Early Eocene climatic, volcanic, and biotic events in the northwestern Tethyan Untersberg section, Austria: Palaeogeography, Palaeoclimatology, Palaeoecology, v. 217, p. 243–264, doi:10.1016/j.palaeo.2004.12.006.

Escarguel, G., Brayard, A., and Bucher, H., 2008, Evolutionary rates do not drive latitudinal diversity gradients: Journal of Zoological Systematics and Evolutionary Research, v. 46, p. 82–86, doi:10.1111/j.1439-0469.2007.00443.x.

Gavrilov, Y.O., Shcherbinina, E.A., and Oberhänsli, H., 2003, Paleocene-Eocene boundary events in the northeastern peri-Tethys, *in* Wing, S.L., Gingerich, P.D., Schmitz, B., and Thomas, E., eds., Causes and Consequences of Globally Warm Climates in the Early Paleogene: Geological Society of America Special Paper 369, p. 147–168.

Gibbs, S.J., Bralower, T.J., Bown, P.R., Zachos, J.C., and Bybell, L.M., 2006, Shelf and open-ocean calcareous phytoplankton assemblages across the Paleocene-Eocene thermal maximum: Implications for global productivity gradients: Geology, v. 34, p. 233–236, doi:10.1130/G22381.1.

Gibbs, S.J., Stoll, H.M., Bown, P.R., and Bralower, T.J., 2010, Ocean acidification and surface water carbonate production across the Paleocene–Eocene thermal maximum: Earth and Planetary Science Letters, v. 295, p. 583–592, doi:10.1016/j.epsl.2010.04.044.

Gibson, T.G., Bybell, L.M., and Owens, J.P., 1993, Latest Paleocene lithologic and biotic events in neritic deposits of southwestern New Jersey: Paleoceanography, v. 8, p. 495–514, doi:10.1029/93PA01367.

Giusberti, L., Rio, D., Agnini, C., Backman, J., Fornaciari, E., Tateo, F., and Oddone, M., 2007, Mode and tempo of the Paleocene-Eocene thermal maximum in an expanded section from the Venetian pre-Alps: Geological Society of America Bulletin, v. 119, p. 391–412, doi:10.1130/B25994.1.

Gradstein, F., Ogg, J., and Smith, A., 2004, A Geologic Time Scale 2004: Cambridge, UK, Cambridge University Press, 589 p.

Hallock, P., 1985, Why are larger foraminifera large?: Palaeobiology, v. 11, no. 2, p. 195–208.

Hallock, P., 2000, Symbiont-bearing foraminifers: Harbingers of global change?: Micropaleontology, v. 46, p. 95–104.

Hallock, P., Premoli Silva, I., and Boersma, A., 1991, Similarities between planktonic and larger foraminifera evolutionary trends through Paleogene paleoceanographic changes: Palaeogeography, Palaeoclimatology, Palaeoecology, v. 83, p. 49–64, doi:10.1016/0031-0182(91)90075-3.

Hallock, P., Lidz, B.H., Cockey-Burkhard, E.M., and Donnelly, K.B., 2003, Foraminifera as bioindicators in coral reef assessment and monitoring: The FORAM index: Environmental Monitoring and Assessment, v. 81, p. 221–238, doi:10.1023/A:1021337310386.

Hedges, J.I., and Keil, R.G., 1995, Sedimentary organic matter preservation: An assessment and speculative synthesis: Marine Chemistry, v. 49, p. 127–136, doi: 10.1016/0304-4203(95)00008-F.

Hottinger, L., 1960, Recherches sur les Alvéolines du Paléocène et de l'Eocène: Mémoires Suisses de Paléontologie 75/76, Birkhäuser (Basel), 243 p.

Hottinger, L., 1982, Larger foraminifera, giant cells with a historical background: Naturwissenschaften, v. 69, p. 361–371, doi:10.1007/BF00396687.

Hottinger, L., 1983, Processes determining the distribution of larger foraminifers in space and time: Utrecht Micropaleontological Bulletin, v. 30, p. 239–253.

Hottinger, L., 1998, Shallow benthic foraminifers at the Paleocene-Eocene boundary: Strata, v. 9, p. 61–64.

Hottinger, L., and Drobne, K., 1980, Early Tertiary conical imperforate foraminifers: Razprave IV: Razreda SAZU, v. 22, p. 186–276.

Hottinger, L., and Schaub, H., 1960, Zur Stufeneinteilung des Paleocaens und des Eocaens. Einführung der Stufen Ilerdien und Biarritzien: Eclogae Geologicae Helvetiae, v. 53, p. 453–480.

Hottinger, L., Smeeni, S.J., and Butt, A.A., 1998, Emendation of *Alveolina vredenburgi* Davies and Pinfold, 1937 from the Surghar Range, Pakistan, *in* Hottinger, L., and Drobne, K., eds., Paleogene Shallow Benthos of the Tethys, 2: Ljubljana, Slovenia, Dela-Opera SAZU, p. 155–163.

Immenhauser, A., Kenter, J.A.M., Ganssen, G., Bahamonde, J.R., Van Vlier, A., and Saher, M.H., 2002, Origin and significance of isotope shifts in Pennsylvanian carbonates (Asturias, NW Spain): Journal of Sedimentary Research, v. 72, p. 82–94, doi:10.1306/051701720082.

Immenhauser, A., Holmden, C., and Patterson, W.P., 2008, Interpreting the carbon-isotope record of ancient shallow epeiric seas: Lessons from the Recent, *in* Pratt, B.R., and Holmden, C., eds., Dynamics of Epeiric Seas: Geological Association of Canada Special Publication 48, p. 135–174.

Jenkyns, H.C., 2003, Evidence for rapid climate change in the Mesozoic-Paleogene greenhouse world: Philosophical Transactions of the Royal Society, Series A, v. 361, p. 1885–1916, doi: 10.1098/rsta.2003.1240.

Joachimski, M., 1994, Subaerial exposure and deposition of shallowing upward sequences: Evidence from stable isotopes of Purbeckian peritidal carbonates (basal Cretaceous), Swiss and French Jura Mountains: Sedimentology, v. 41, p. 805–824, doi:10.1111/j.1365-3091.1994.tb01425.x.

John, C.M., Bohaty, S.M., Zachos, J.C., Sluijs, A., Gibbs, S., Brinkhuis, H., and Bralower, T.J., 2008, North American continental margin records of the Paleocene-Eocene thermal maximum: Implications for global carbon and hydrological cycling: Paleoceanography, v. 23, doi:10.1029/2007PA001465.

Jurkovšek, B., 2010, Geološka karta severnega dela Tržaško-komenske planote 1:25.000 (Geological Map of the northern part of the Trieste-Komen Plateau 1:25,000): Ljubljana, Slovenia, Geološki zavod Slovenije.

Jurkovšek, B., Toman, M., Ogorelec, B., Šribar, L., Drobne, K., Poljak, M., and Šribar, L.J., 1996, Formacijska geološka karta južnega dela Tržaško-komenske planote 1:50.000. Kredne in paleogenske karbonatne kamnine: Ljubljana, Slovenia, Inštitut za Geologijo, Geotehniko in Geofiziko, 143 p.

Kennett, J.P., and Stott, L.D., 1991, Abrupt deep-sea warming, palaeoceanographic changes and benthic extinctions at the end of the Palaeocene: Nature, v. 353, p. 225–229, doi:10.1038/353225a0.

Kiessling, W., and Simpson, C., 2011, On the potential for ocean acidification to be a general cause of ancient reef crises: Global Change Biology, v. 17, p. 56–67, doi:10.1111/j.1365-2486.2010.02204.x.

Košir, A., 1997, Eocene platform-to-basin depositional sequence, southwestern Slovenia: Gaea Heidelbergiensis, v. 3, p. 205.

Košir, A., 2003, Litostratigrafska revizija zgornje krede in paleogena v jugozahodni Sloveniji: Geološki Zbornik (Ljubljana), v. 17, p. 92–98.

Košir, A., 2004, *Microcodium* revisited: Root calcification products of terrestrial plants on carbonate-rich substrates: Journal of Sedimentary Research, v. 74, p. 845–857, doi:10.1306/040404740845.

Kump, L.R., Bralower, T.J., and Ridgwell, A., 2009, Ocean acidification in deep time: Oceanography (Washington, D.C.), v. 22, p. 94–107, doi:10.5670/oceanog.2009.100.

Langer, M., 1995, Oxygen and carbon isotopic composition of Recent and larger and smaller foraminifera from the Madang Lagoon (Papua New Guinea): Marine Micropaleontology, v. 26, p. 215–221, doi:10.1016/0377-8398(95)00073-9.

Langer, M., and Hottinger, L., 2000, Biogeography of selected "larger" foraminifers: Micropaleontology, v. 46, p. 105–126.

Magioncalda, R., Dupuis, C., Smith, T., Steurbaut, E., and Gingerich, P.D., 2004, Paleocene-Eocene carbon isotope excursion in organic carbon and pedogenic carbonate: Direct comparison in a continental stratigraphic section: Geology, v. 32, p. 553–556, doi:10.1130/G20476.1.

Orue-Etxebarria, X., Pujalte, V., Bernaola, G., Apellaniz, E., Baceta, J.I., Payros, A., Nunez-Betelu, K., Serra-Kiel, J., and Tosquella, J., 2001, Did the late Paleocene thermal maximum affect the evolution of larger foraminifers? Evidence from calcareous plankton of the Campo Section (Pyrenees, Spain): Marine Micropaleontology, v. 41, p. 45–71, doi:10.1016/S0377-8398(00)00052-9.

Pagani, M., Pedentchouk, N., Huber, M., Sluijs, A., Schouten, S., Brinkhuis, H., Sinninghe Damsté, J.S., Dickens, G.R., and Expedition Scientists, 2006, Arctic hydrology during global warming at the Palaeocene-Eocene thermal maximum: Nature, v. 442, p. 671–675, doi:10.1038/nature05043.

Patterson, W.P., and Walter, L.M., 1994a, Syndepositional diagenesis of modern platform carbonates: Evidence from isotopic and minor element data: Geology, v. 22, p. 127–130, doi:10.1130/0091-7613(1994)022<0127:SDOMPC>2.3.CO;2.

Patterson, W.P., and Walter, L.M., 1994b, Depletion of ^{13}C in seawater ΣCO_2 on modern carbonate platforms: Significance for the carbon isotope record of carbonates: Geology, v. 22, p. 885–888, doi:10.1130/0091-7613(1994)022<0885:DOCISC>2.3.CO;2.

Pomar, L., 2001, Types of carbonate platforms: A genetic approach: Basin Research, v. 13, p. 313–334, doi:10.1046/j.0950-091x.2001.00152.x.

Pujalte, V., Orue-Etxebarria, X., Schmitz, B., Tosquella, J., Baceta, J.I., Payros, A., Bernaola, G., Caballero, F., and Apellaniz, E., 2003a, Basal Ilerdian (earliest Eocene) turnover of larger foraminifers: Age constraints based on calcareous plankton and $\delta^{13}C$ isotopic profiles from new southern Pyrenean sections (Spain), *in* Wing, S.L., Gingerich, P.D., Schmitz, B., and Thomas, E., eds., Causes and Consequences of Globally Warm Climates in the Early Paleogene: Geological Society of America Special Paper 369, p. 205–221.

Pujalte, V., Dinarès-Turell, J., Bernaola, G., Baceta, J.I., and Payros, A., 2003b, A reappraisal of the position of Chron C25n in the Campo section (Huesca province, south-central Pyrenees): Geogaceta, v. 34, p. 155–158.

Pujalte, V., Schmitz, B., Baceta, J.I., Orue-Etxebarria, X., Bernaola, G., Dinarès-Turel, J., Payros, A., Apellániz, E., and Caballero, F., 2009, Correlation of the Thanetian-Ilerdian turnover of larger foraminifera and the Paleocene-Eocene thermal maximum: Confirming evidence from the Campo area (Pyrenees, Spain): Geologica Acta, v. 7, p. 161–175.

Ravizza, G., Norris, R.N., Blusztajn, J., and Aubry, M.-P., 2001, An osmium isotope excursion associated with the late Paleocene thermal maximum: Evidence of intensified chemical weathering: Paleoceanography, v. 16, p. 155–163, doi:10.1029/2000PA000541.

Ridgwell, A., and Schmidt, D.N., 2010, Past constraints on the vulnerability of marine calcifiers to massive carbon dioxide release: Nature Geoscience, v. 3, p. 196–200, doi:10.1038/ngeo755.

Robinson, S.A., 2011, Shallow-water carbonate record of the Paleocene Eocene thermal maximum from a Pacific Ocean guyot: Geology, v. 39, p. 51–54, doi:10.1130/G31422.1.

Röhl, U., Bralower, T.J., Norris, R.D., and Wefer, G., 2000, New chronology for the late Paleocene thermal maximum and its environmental implications: Geology, v. 28, p. 927–930, doi:10.1130/0091-7613(2000)28<927:NCFTLP>2.0.CO;2.

Röhl, U., Westerhold, T., Bralower, T.J., and Zachos, J.C., 2007, On the duration of the Paleocene–Eocene thermal maximum (PETM): Geochemistry, Geophysics, Geosystems, v. 8, p. 1–13, doi:10.1029/2007GC001784.

Sanders, D., 2003, Syndepositional dissolution of calcium carbonate in neritic carbonate environments: Geological recognition, processes, potential significance: Journal of African Earth Sciences, v. 36, p. 99–134, doi:10.1016/S0899-5362(03)00027-7.

Schaub, H., 1981, Nummulites et Assilines de la Téthys paléogène. Taxinomie, phylogenèse et biostratigraphie: Mémoires Suisses de Paléontologie, v. 104/105/106, Birkhäuser (Basel), 236 p.

Scheibner, C., and Speijer, R.P., 2009, Recalibration of the Tethyan shallow-benthic zonation across the Paleocene-Eocene boundary; the Egyptian record: Geologica Acta, v. 7, p. 195–214.

Scheibner, C., Speijer, R.P., and Marzouk, A.M., 2005, Turnover of larger foraminifers during the Paleocene-Eocene thermal maximum and paleoclimatic control on the evolution of platform ecosystems: Geology, v. 33, p. 493–496, doi:10.1130/G21237.1.

Schmitz, B., and Pujalte, V., 2003, Sea-level, humidity, and land-erosion records across the initial Eocene thermal maximum from a continental-marine transect in northern Spain: Geology, v. 31, p. 689–692, doi:10.1130/G19527.1.

Schmitz, B., and Pujalte, V., 2007, Abrupt increase in seasonal extreme precipitation at the Paleocene-Eocene boundary: Geology, v. 35, p. 215–218, doi:10.1130/G23261A.1.

Serra-Kiel, J., Hottinger, L., Caus, E., Drobne, K., Ferrandez, C., Jauhri, A.K., Less, G., Pavlovec, R., Pignatti, J., Samso, J.M., Schaub, H., Sirel, E., Strougo, A., Tambareau, Y., Tosquella, J., and Zakrevskaya, E., 1998, Larger foraminiferal biostratigraphy of the Tethyan Paleocene and Eocene: Bulletin de la Société Géologique de France, v. 169, p. 281–299.

Sluijs, A., and Brinkhuis, H., 2009, A dynamic climate and ecosystem state during the Paleocene-Eocene thermal maximum: Inferences from dinoflagellate cyst assemblages on the New Jersey shelf: Biogeosciences, v. 6, p. 1755–1781, doi:10.5194/bg-6-1755-2009.

Speijer, R.P., and Wagner, T., 2002, Sea-level changes and black shales associated with the late Paleocene thermal maximum: Organic-geochemical and micropaleontological evidence from the southern Tethyan margin (Egypt-Israel), *in* Koeberl, C., and MacLeod, K.G., eds., Catastrophic events and mass extinctions: Impacts and beyond: Geological Society of America Special Paper 356, p. 533–549.

Swart, P.K., and Eberli, G., 2005, The nature of the $\delta^{13}C$ of periplatform sediments: Implications for stratigraphy and the global carbon cycle: Sedimentary Geology, v. 175, p. 115–129, doi:10.1016/j.sedgeo.2004.12.029.

Thomas, D.J., Zachos, J.C., Bralower, T.J., Thomas, E., and Bohaty, S., 2002, Warming the fuel for the fire: Evidence for the thermal dissociation of methane hydrate during the Paleocene-Eocene thermal maximum: Geology, v. 30, p. 1067–1070, doi:10.1130/0091-7613(2002)030<1067:WTFFTF>2.0.CO;2.

Thomas, E., 1998, Biogeography of the late Paleocene benthic foraminifera extinction, *in* Aubry, M.-P., Lucas, S., and Berggren, W.A., eds., Late Paleocene–early Eocene climatic and biotic events in the marine and terrestrial records: New York, Columbia University Press, p. 214–243.

Thomas, E., 2007, Cenozoic mass extinctions in the deep sea: What perturbs the largest habitat on Earth?, *in* Monechi, S., Coccioni, R., and Rampino, M., eds., Large Ecosystem Perturbations: Causes and Consequences: Geological Society of America Special Paper 424, p. 1–24.

Toler, S.K., and Hallock, P., 1998, Shell malformation in stressed *Amphistegina* populations: Relation to biomineralization and paleoenvironmental potential: Marine Micropaleontology, v. 34, p. 107–115, doi:10.1016/S0377-8398(97)00043-1.

Tripati, A.K., and Elderfield, H., 2005, Deep-sea temperature and circulation changes at the Paleocene-Eocene thermal maximum: Science, v. 308, p. 1894–1898, doi:10.1126/science.1109202.

Weissert, H.J., McKenzie, J.A., and Channel, J.E.T., 1985, Natural variations in the carbon cycle during the Early Cretaceous, *in* Sundquist, E.T., and Broeker, W.S., eds., The Carbon Cycle and Atmospheric CO_2: Natural Variations Archean to Present: American Geophysical Union Geophysical Monograph 32, p. 531–546.

Zachos, J., Pagani, M., Sloan, L., Thomas, E., and Billups, K., 2001, Trends, rhythms, and aberrations in global climate 65 Ma to present: Science, v. 292, p. 686–693, doi:10.1126/science.1059412.

Zachos, J.C., Wara, M.W., Bohaty, S., Delaney, M.L., Rose-Petrizzo, M., Brill, A., Bralower, T.J., and Premoli-Silva, I., 2003, A transient rise in tropical sea surface temperature during the Paleocene-Eocene thermal maximum: Science, v. 302, p. 1551–1554, doi:10.1126/science.1090110.

Zachos, J.C., Röhl, U., Schellenberg, S.A., Sluijs, A., Hodell, D.A., Kelly, D.C., Thomas, E., Nicolo, M., Raffi, I., Lourens, L.J., McCarren, H., and Kroon, D., 2005, Rapid acidification of the ocean during the Paleocene-Eocene thermal maximum: Science, v. 308, p. 1611–1615, doi:10.1126/science.1109004.

Zachos, J.C., Schouten, S., Bohaty, S., Quattlebaum, T., Sluijs, A., Brinkhuis, H., Gibbs, S.J., and Bralower, T.J., 2006, Extreme warming of mid latitude coastal ocean during the Paleocene-Eocene thermal maximum: Inferences from TEX86 and isotope data: Geology, v. 34, p. 737–740, doi:10.1130/G22522.1.

Zachos, J.C., Dickens, G.R., and Zeebe, R.E., 2008, An early Cenozoic perspective on greenhouse warming and carbon-cycle dynamics: Nature, v. 451, p. 279–283, doi:10.1038/nature06588.

Zamagni, J., Mutti, M., and Košir, A., 2008, Paleoecology of larger foraminifers during the late Paleocene–earliest Eocene transition in the northern Tethys (SW Slovenia): Facies, v. 54, p. 25–43, doi:10.1007/s10347-007-0123-3.

Zamagni, J., Košir, A., and Mutti, M., 2009, The first microbialite-coral mounds in the Cenozoic (uppermost Paleocene) from the northern Tethys (Slovenia): Environmentally-triggered phase shifts preceding the PETM?: Palaeogeography, Palaeoclimatology, Palaeoecology, v. 274, p. 1–17, doi:10.1016/j.palaeo.2008.12.007.

Zamagni, J., Mutti, M., and Košir, A., 2012, The evolution of mid Paleocene–early Eocene coral communities: How to survive during rapid global warming: Palaeogeography, Palaeoclimatology, Palaeoecology, v. 317–318, p. 48–65, doi:10.1016/j.palaeo.2011.12.010.

Ziegler, P.A., 1990, Geological Atlas of Western and Central Europe (2nd ed.): The Hague, Netherlands, Shell Petroleum Maatschappig BV.

Science Editor: Christian Koeberl
Associate Editor: Brian R. Pratt

Manuscript Received 22 May 2011
Revised Manuscript Received 4 February 2012
Manuscript Accepted 7 February 2012

Printed in the USA